

AD-782 814

TEST RESULTS AND TECHNOLOGY DEVELOPMENT REPORT: HLH/ATC (HEAVY LIFT HELICOPTER/ADVANCED TECHNOLOGY COMPONENT) TRANSMISSION OVERRUNNING CLUTCH

Nelson J. Ayoub, et al

Boeing Vertol Company

Prepared for:

Army Air Mobility Research and Development Laboratory

April 1974

DISTRIBUTED BY:

NTIS

National Technical Information Service
U. S. DEPARTMENT OF COMMERCE
5285 Port Royal Road, Springfield Va. 22151

Unclassified

SECURITY CLASSIFICATION OF THIS PAGE (When Data Entered)

AD 782 814

REPORT DOCUMENTATION PAGE		READ INSTRUCTIONS BEFORE COMPLETING FORM
1. REPORT NUMBER USAAMRDL-TR-74-17	2. GOVT ACCESSION NO.	3. RECIPIENT'S CATALOG NUMBER
4. TITLE (and Subtitle) Test Results and Technology Development Report--HLH/ATC Transmission Overrunning Clutch		5. TYPE OF REPORT & PERIOD COVERED
7. AUTHOR(s) Nelson J. Ayoub W. G. Perin		6. PERFORMING ORG. REPORT NUMBER T301-10222-1
9. PERFORMING ORGANIZATION NAME AND ADDRESS Boeing Vertol Company, A Division of The Boeing Company, P. O. Box 16858 Philadelphia, Pennsylvania 19142		8. CONTRACT OR GRANT NUMBER(s) DAAJ01-71-C-0840 (P40)
11. CONTROLLING OFFICE NAME AND ADDRESS U. S. Army Aviation Systems Command P.O. Box 209, Main Office St. Louis, Missouri 63166		10. PROGRAM ELEMENT, PROJECT, TASK AREA & WORK UNIT NUMBERS
14. MONITORING AGENCY NAME & ADDRESS (if different from Controlling Office) Eustis Directorate, U.S. Army Air Mobility Research and Development Laboratory Fort Eustis, Virginia 23604		12. REPORT DATE April 1974
		13. NUMBER OF PAGES 96
		15. SECURITY CLASS. (of this report) Unclassified
		15a. DECLASSIFICATION/DOWNGRADING SCHEDULE
16. DISTRIBUTION STATEMENT (of this Report) Approved for public release; distribution unlimited.		
17. DISTRIBUTION STATEMENT (of the abstract entered in Block 20, if different from Report)		
18. SUPPLEMENTARY NOTES		
19. KEY WORDS (Continue on reverse side if necessary and identify by block number) Heavy lift helicopter Clutches Drives		
20. ABSTRACT (Continue on reverse side if necessary and identify by block number) This report presents the results of an evaluation test program to develop the optimum sprag engine/transmission clutch for use in the Heavy Lift Helicopter (HLH) drive system. The design operating conditions were 3,795 ft-lb of torque transmitted at 11,500 rpm. Three clutch configurations with differing design philosophies were first subjected to a preliminary evaluation;		

DD FORM 1 JAN 73 1473 EDITION OF 1 NOV 65 IS OBSOLETE

Reproduced by
NATIONAL TECHNICAL
INFORMATION SERVICE
U. S. Department of Commerce
Springfield, VA 22151

Unclassified
SECURITY CLASSIFICATION OF THIS PAGE (When Data Entered)

Unclassified

SECURITY CLASSIFICATION OF THIS PAGE(When Data Entered)

Block 20. Abstract - continued.

- Borg-Warner Xl37661--Design A
- Borg-Warner Xl37675--Design B
- Formsprag CL-41802--Design C

As a result of this preliminary evaluation consisting of over-running and differential-speed testing, the Borg-Warner design Xl37675 was judged to have the best performance. Accordingly, this design was then optimized (Borg-Warner design Xl37920, Design D) and subjected to a more comprehensive test program:

- Full-Speed Dynamic Clutch-Overrun Testing
- Differential-Speed Clutch-Overrun Testing
- Static Cyclic Torque Fatigue Testing
- Static Overload Testing
- 50-Hour Endurance Testing

Drag torque, oil temperatures, and oil flow were monitored during the dynamic testing.

The optimized Design D Borg-Warner Xl37920 clutch configuration successfully met all HLH Advanced Technology Component (ATC) design requirements.

ia

Unclassified

SECURITY CLASSIFICATION OF THIS PAGE(When Data Entered)


Eustis Directorate Position Statement

The objective of this effort was to conduct an extensive test and evaluation program to develop an optimum sprag clutch for use in the Heavy Lift Helicopter (HLH) drive system.

The clutch configurations tested incorporated many of the design recommendations published in USAAMRD Technical Report 72-49, "Sprag Overriding Aircraft Clutch". As a result of these recommendations and those generated during the program, a successful clutch design evolved. The resulting clutch configuration was thoroughly tested and met all the HLH drive system design requirements.

This directorate concurs with the conclusions presented herein.

The technical monitor for this effort was Mr. Wayne A. Hudgins, Heavy Lift Helicopter Project Office, Systems Support Division.

ADDITIONAL FOR		WHITE SECTION
NTIS		
D.O.		ENCL. SECTION
ORAL. COVER		<input type="checkbox"/>
JUSTIFICATION		<input type="checkbox"/>
BY		
DISTRIBUTION/AVAILABILITY CODES		
DISL.	AVAIL.	ENCL. SPECIAL
		

DISCLAIMERS

The findings in this report are not to be construed as an official Department of the Army position unless so designated by other authorized documents.

When Government drawings, specifications, or other data are used for any purpose other than in connection with a definitely related Government procurement operation, the United States Government thereby incurs no responsibility nor any obligation whatsoever; and the fact that the Government may have formulated, furnished, or in any way supplied the said drawings, specifications, or other data is not to be regarded by implication or otherwise as in any manner licensing the holder or any other person or corporation, or conveying any rights or permission, to manufacture, use, or sell any patented invention that may in any way be related thereto.

Trade names cited in this report do not constitute an official endorsement or approval of the use of such commercial hardware or software.

DISPOSITION INSTRUCTIONS

Destroy this report when no longer needed. Do not return it to the originator.

PREFACE

The program was conducted from August 1972 through April 1973 for the U.S. Army Aviation Systems Command, St. Louis, Missouri, under Contract DAAJ01-71-C-0840(P40).

Acknowledgment is made to the engineering staffs of the following organizations for their assistance in the design, fabrication, and evaluation of the clutches used in this program:

- Spring Division, Borg-Warner Corporation,
Bellwood, Illinois.
- Formsprag Company,
Warren, Michigan.

U.S. Army technical direction was provided by Wayne A. Hudgins and Dom Lubrano of the Eustis Directorate, U.S. Army Air Mobility Research and Development Laboratory, Ft. Eustis, Virginia.

TABLE OF CONTENTS

	<u>Page</u>
PREFACE	iii
LIST OF ILLUSTRATIONS	vi
LIST OF TABLES	ix
HLH CLUTCH DESIGN	1
Sprag-Clutch Operation	2
HLH Sprag-Clutch Design Criteria	3
DESCRIPTION OF TEST CLUTCHES	5
TEST FACILITY	22
Dynamic Tests	22
Static Test	28
TEST PROCEDURE	33
General	33
Full-Speed Overrun Test	33
Differential-Speed Overrun Test	34
Static Overload Test	35
Nonrotating Cyclic-Torque Slip Test	35
Static Cyclic-Torque Fatigue Test	36
50-Hour Differential-Speed Endurance Test	36
TEST DISCUSSION AND RESULTS	37
Initial Checkout of Fixture	37
Determination of Optimum Design	37
Design A Clutch (Borg-Warner X137661)	37
Design B (Borg-Warner X137675)	42
Design C (Formsprag CL-41802)	47
Testing of Optimized Design D	49
Static Overload Test	63
Clutch Analysis	73
CONCLUSIONS	80
APPENDIX: Sprag-Clutch Analysis	81
LIST OF SYMBOLS	89

Preceding page blank

LIST OF ILLUSTRATIONS

<u>Figure</u>		<u>Page</u>
1	HLH Drive System	1
2	Principle of Sprag-Clutch Operation	2
3	HLH/ATC Sprag-Clutch Designs	5
4	Design A--Borg-Warner X137661	7
5	Design B--Borg-Warner X137675	8
6	Design C--Formsprag CL-41802	9
7	Optimized Design D--Borg-Warner X137920	10
8	Shaft Fatigue, Static, and Override Clutch Test--Engineering Drawing	11
9	Housing Clutch Test--Engineering Drawing	13
10	Inner Clutch Shaft of Combiner Transmission-- Engineering Drawing	15
11	Engine Clutch Shaft of Combiner Transmission-- Engineering Drawing	19
12	Combiner Transmission for the Heavy-Lift Transmissions.	21
13	Dynamic Clutch-Test Facility	23
14	Clutch-Test Fixture Variable-Speed Overrun Subassembly	25
15	Clutch-Test Lubrication System	27
16	Acurex 1206 Telemetric Drag-Torque Readout System	28
17	Dynamic Test-Specimen Cartridge and Acurex Telemetry System	29
18	Clutch Cyclic Torque Test	30
19	Fatigue and Static Clutch-Test Assembly	31
20	Cracking of Tapered-Roller Bearing--Initial Assembly	38

<u>Figure</u>		<u>Page</u>
21	Surface Damage of Tapered-Roller Bearing	39
22	Wear on Outside Diameter of Design A Drag Strips	40
23	Design A Components After 50-Percent Differential-Speed Overrun Test	41
24	Heat Rejection Versus Oil Flow at 100-Percent Overrunning	44
25	Drag Torque Versus Oil Flow at 100-Percent Overrunning	44
26	Heat Rejection Versus Differential Speed Overrunning	45
27	Drag Torque Versus Differential Speed	46
28	Design B Clutch Shaft Exhibiting 0.0016-Inch Wear on Inner Race After Disengagement Test . .	47
29	Design C Components After 75-Percent Differential-Speed Overrun Test	48
30	Design C Inner Race After Differential-Speed Test With Low Center-of-Gravity Offset Sprags .	48
31	Summary of Clutch-Evaluation Testing	50
32	Clutches and Inner-Race Shafts After Evaluation Testing	51
33	Design D Inner Drag Strip, Showing No Wear After 50-Hour Endurance Test	52
34	Design D Outer Drag Strip, Showing No Wear After 50-Hour Endurance Test	53
35	Map of Failures of Design A Energizing Ribbon After 50-Hour Endurance Testing	55
36	Map of Failures of Design D Energizing Ribbon After 50-Hour Endurance Testing	55
37	Design D Inner Race, Showing No Wear After 50-Hour Endurance Test	56
38	Results of Slip Test	56

<u>Figure</u>		<u>Page</u>
39	Results of the Nonrotating Cyclic-Torque Fatigue Test	57
40	Design A Cage Damage From Fatigue Testing	58
41	Clutch-Shaft Fatigue Damage	59
42	Clutch-Housing Fatigue Damage	60
43	Cracks on Outer Cage After Nonrotating Cyclic-Torque Fatigue Test--Assembly Similar to Design D	61
44	Cracks on Inner Cage After Nonrotating Cyclic-Torque Fatigue Test--Assembly Similar to Design D	62
45	Instrumentation for Sprag-Clutch Load-Sharing Static Test	65
46	Load-Sharing Measurement Scheme	67
47	Results of Load-Sharing Clutch Test--T-1 Torque Bridge	69
48	Results of Load-Sharing Clutch Test--T-2 Torque Bridge	69
49	Design D Components After Static Overload Test	71
50	Inner-Race Contact Stress Versus Clutch Torque	75
51	Outer-Race Hoop Stress Versus Clutch Torque	76
52	Inner-Race Strut Angle Versus Clutch Torque	77
53	Percentage of Cam Rise Versus Inner-Race Strut Angle	78
54	Sprag Geometry	81

LIST OF TABLES

<u>Table</u>		<u>Page</u>
I	Conditions for the Full-Speed Overrun Test . . .	33
II	Conditions for the Differential-Speed Overrun Test	34
III	Summary of Optimization Testing	43
IV	Load-Sharing Calibration--Row 1 Only	67
V	Load-Sharing Calibration--Row 2 Only	68
VI	Results of Load-Sharing Test	68
VII	Housing Radial Deflection	70
VIII	Summary of Load-Sharing Test Results	72
IX	Clutch Geometry	74
X	Comparison of Design D and Aircraft Clutch Parameters With Design Criteria	79

HLH CLUTCH DESIGN

Reference 1 describes a program to advance the technology of overrunning sprag-clutch units to allow for reliable and efficient operation at speeds and loads commensurate with advanced aircraft gas-turbine engines.

The test program described in Reference 2 applies the knowledge gained to develop an overrunning clutch capable of meeting the HLH design requirements. The design operating conditions for this program were 11,500 rpm and 3,795 ft-lb torque.

The overrunning clutch is a critical helicopter component that transmits engine torque in normal operation and allows the rotors to autorotate in case of engine malfunction. With the advent of multiengine configurations, the overrunning clutch assumes an even greater role, since the aircraft must be capable of operation with an engine shut down or with engines operating at different speeds. To achieve the lightest configuration, the overrun clutch is located on the high-speed shaft before the first gear reduction. Figure 1 shows a schematic of the HLH drive system and lists the design ratings.

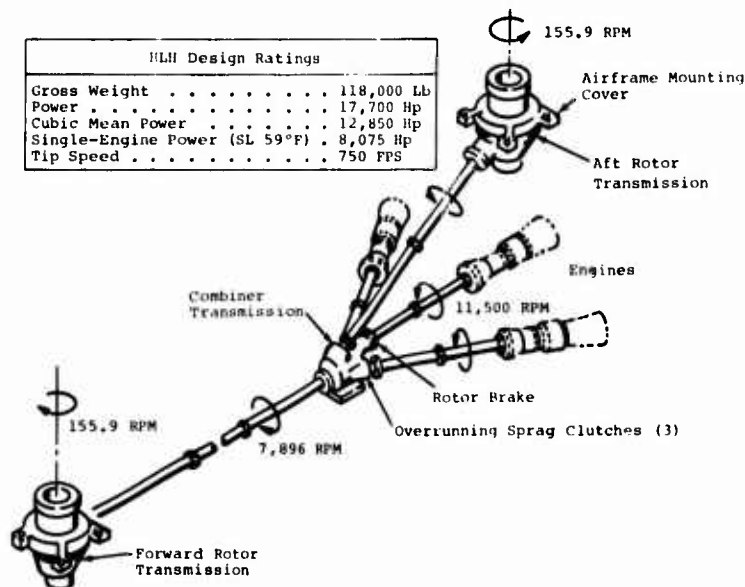


Figure 1. HLH Drive System.

¹Lynwander, P., Meyer, A. G., and Chachakis, S., SPRAG OVER AIRCRAFT CLUTCH, USAAMRDL Technical Report 72-49, U.S. Army Air Mobility Research and Development Laboratory, Fort Eustis, Virginia, July 1972, AD747807.

²Boeing Vertol Test Plan--HLH/ATC Transmission Overrunning Clutch Development Program, D301-10118-1.

SPRAG-CLUTCH OPERATION

The principle of sprag-clutch operation is illustrated in Figure 2. The sprag component is designed with cross-corner dimensions such that $a > b$. Assuming that an engine is driving counterclockwise through the outer race, the wedging action of the sprag (contact through dimension a) will drive a gearbox through the inner race. If the engine is shut down and the gearbox continues to rotate, the clutch will overrun (sprags rotate clockwise toward dimension b), thus achieving the desired effect of disengaging the engine and its associated drag torque from the drive system.

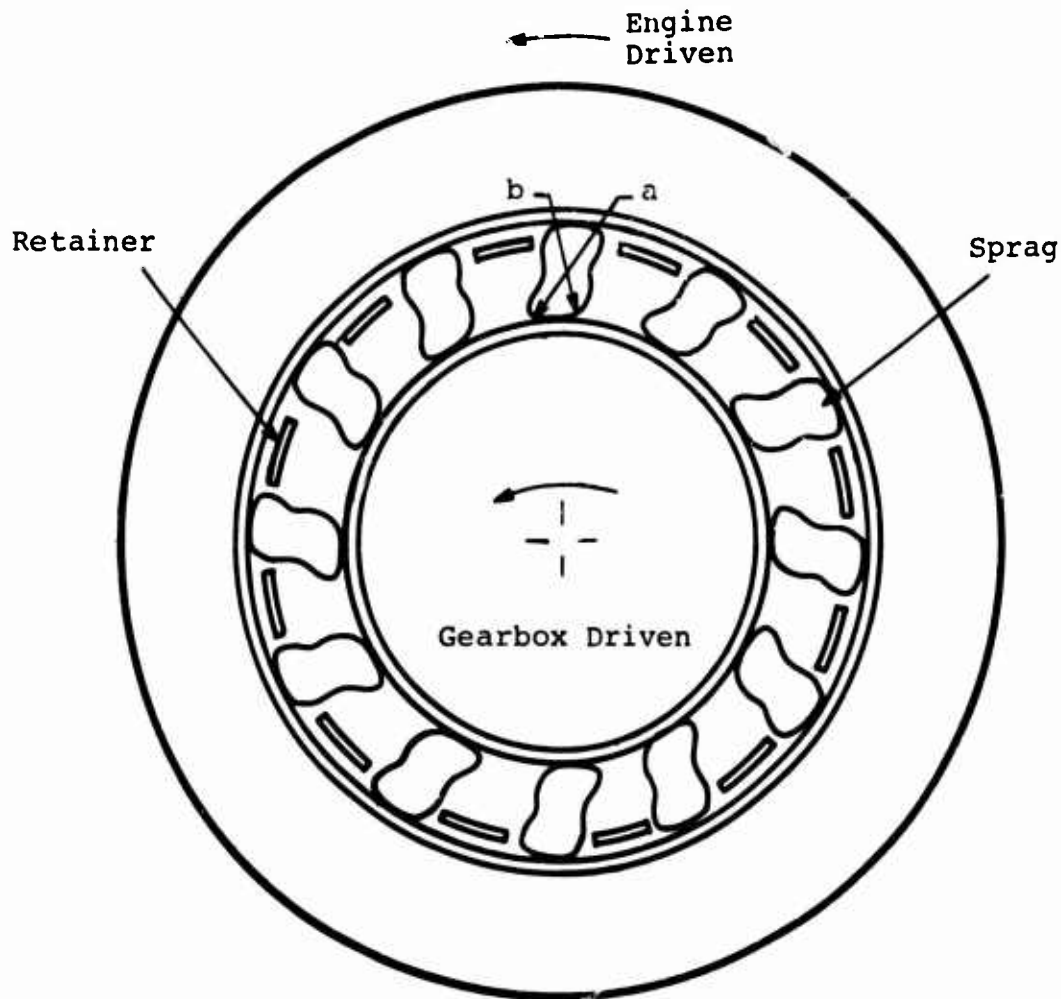


Figure 2. Principle of Sprag-Clutch Operation.

A spring is normally added to the clutch to ensure traction (energizing) during driving, and to maintain raceway contact during overrunning. To provide for equal load sharing (full phasing), a retainer is employed between the races to keep the sprags uniformly spaced. A centrifugal force produced by the mass and rotation of the sprags also acts to energize the clutch during the engine-drive mode. No centrifugal force acts on the sprags during the 100-percent overrunning mode because the tangential driving force component is greater at the inner race so slipping occurs initially at the inner race and the sprags remain stationary with the outer race.

An important feature of sprag-cam design is the compounding of radii of curvature, especially at the inner race. When the clutch changes from the load to overrun mode of operation (called the release position), the radius of curvature at the inner race is greatly reduced, thus allowing the clutch to slip more easily into the overrun mode.

In addition to the conditions just described--drive and overrunning--a third mode of operation, called differential speed, must be evaluated. In a multiengine application, if one engine is driving the gearbox, the clutches on the other engines are overrunning: the inner races are coupled to the gearbox and are rotating at speed of the first engine. If a second engine is started, it cannot transmit torque to the gearbox until it accelerates to the speed of the first engine. During this time, however, centrifugal force of the sprags acts to energize the clutch; this condition is much more severe on the wear life of the clutch than pure overrunning. This mode of operation could occur during preflight checkout of the aircraft or during flight if one engine is driving and the other is maintained at idle for quick response to any need for reserve power.

HLH SPRAG-CLUTCH DESIGN CRITERIA

- Single-engine torque is 3,795 ft-lb (100 percent) at 11,500 rpm. Engine rotation is clockwise looking forward.
- Sprag-clutch torque capacity must be 7,590 ft-lb (200 percent) minimum based on a contact stress of 450,000 psi.
- No permanent deformation or yield of shaft, springs, or cage may occur at 11,386 ft-lb (300 percent) based on a contact tact stress of 600,000 psi.
- No structural failure, overturning, or slippage may occur at 17,078 ft-lb (450 percent).
- Outer-race hoop stress may not exceed 71,200 psi (Rc 36 hardness minimum) at a torque of 7,590 ft-lb (200 percent).

- Combined radial deflection of inner shaft, outer shaft, sprag contacts, and sprag may not exceed 80 percent of sprag total cam rise for torque load of 7,590 ft-lb (200 percent).
- The clutch shall be capable of continuous operation at two-thirds differential overrun (outer race at 7,667 rpm and inner race at 11,500 rpm). Both rotations are clockwise looking at input end of outer shaft.
- Sprags must be made from M-50 steel or equivalent.
- Cages must be fully machined and hardened.
- Positive lubrication shall be provided to the clutch with oil dams to keep sprags submerged in oil during operation. Oil drains must be included in the outer shaft to prevent sludging. Total oil flow is not required to pass through adjacent clutch bearings.
- Clutch-shaft material must be XBMN-7-223 (Vasco) carburized with no black oxide on clutch surface.
- Surface finish must be as follows: inner and outer clutch-shaft diameters, 8 to 16 RHR; sprags, 4 to 8 RHR.

DESCRIPTION OF TEST CLUTCHES

Three clutch configurations were given a preliminary evaluation. These designs were designated as clutch designs A, B, and C and are shown in Figure 3. As a result of these preliminary tests, Design B was judged to have the best performance. The selected configuration was then optimized to eliminate the discrepancies which occurred during the preliminary evaluation and designated as optimized Design D. Finally, the optimized Design D underwent an extensive test program which demonstrated satisfactory performance in meeting HLH design requirements.

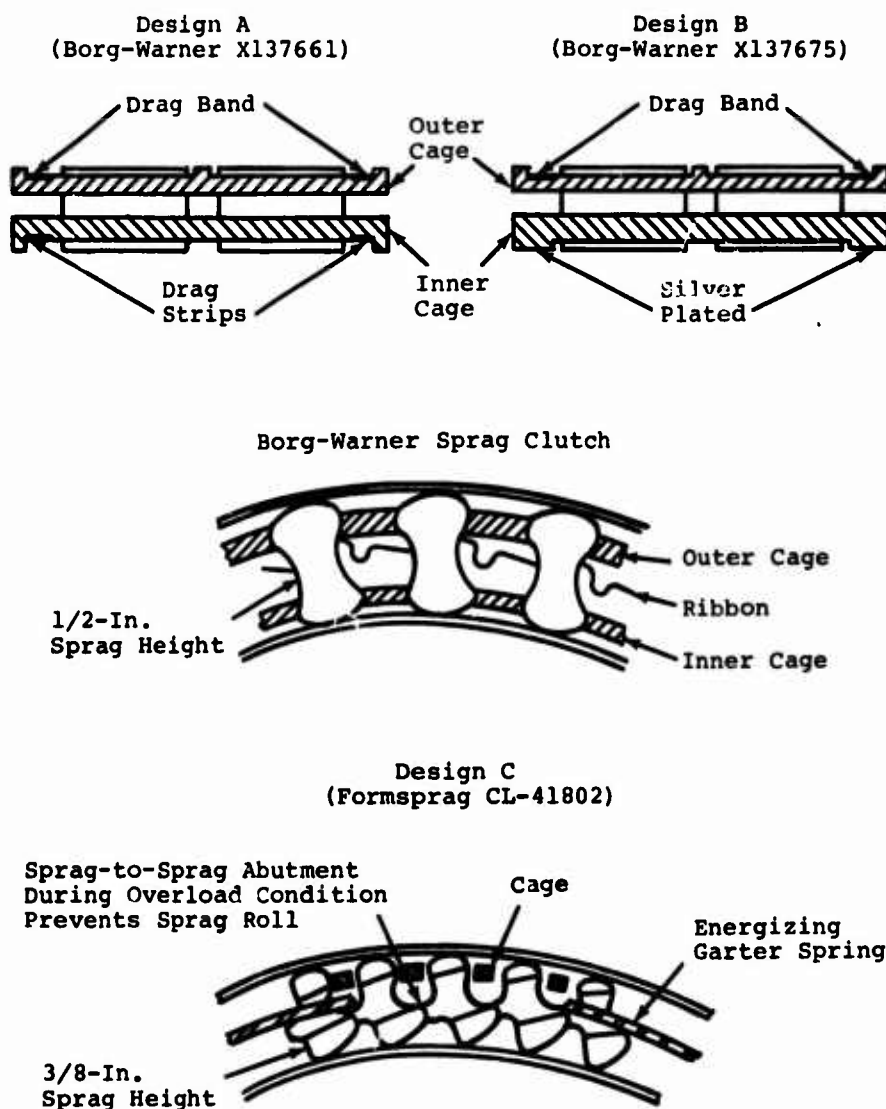


Figure 3. HLH/ATC Sprag-Clutch Designs.

Design A, Borg-Warner X137661, is a two-row sprag-clutch assembly with tandem inner and outer cages incorporating two inner and two outer drag strips and a central energizing ribbon. Design A is shown in Figure 4.

Design B, Borg-Warner X137675, is a two-row sprag-clutch assembly with a tandem inner and outer cage incorporating two outer drag strips but no inner drag strip. Silver-plated lands on the inner cage pilot closely to the inner shaft and use viscous drag to actuate the cage. Design B is shown in Figure 5.

The function of the drag strips in all cases is to create frictional drag between the sprag assembly and the adjacent inner and/or outer races, thereby aiding in the assembly cage actuation.

Design C, Formsprag CL-41802, consists of two single-row sprag-clutch assemblies, each having a cage and two garter springs to locate and actuate the sprags. The sprags have interlocking surfaces which prevent rollover when an overload condition occurs. Figure 6 shows Design C.

Optimized Design D, Borg-Warner X137920, is similar to Design A in appearance and Design B in configuration except for optimization to eliminate minor discrepancies which occurred during the preliminary evaluation. The design consists of a two-row sprag-clutch assembly with a tandem inner and outer cage incorporating two inner and two outer drag strips. Silver-plated lands on the inner cage pilot closely to the inner shaft. The race-contact surface of the outer drag strips were increased to minimize wear. Figure 7 shows the Design D clutch tested.

Lubrication to the clutch designs tested was provided centrifugally via holes drilled through the inner shaft (race), shown in Figure 8. Figure 9 shows the outer test housing within which the test clutch was mounted.

Figure 10 shows the final HLH/ATC sprag-clutch design, part 301-10629, and Figure 11 shows the final HLH/ATC inner clutch-shaft design, Boeing part 301-10646, resulting from this program for incorporation into the HLH/ATC combiner transmission. These final HLH/ATC parts are identical to the optimum Design D tested. Figure 12, an excerpt from Boeing drawing 301-10600, the combiner-transmission assembly, is also included to show the typical arrangement of the sprag clutch in the HLH transmission.

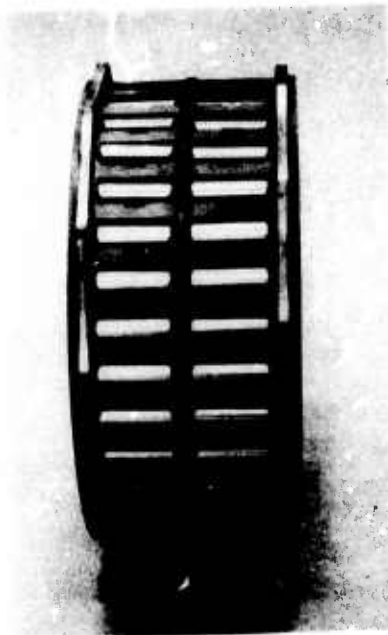


Figure 4. Design A--Borg-Warner X137661.

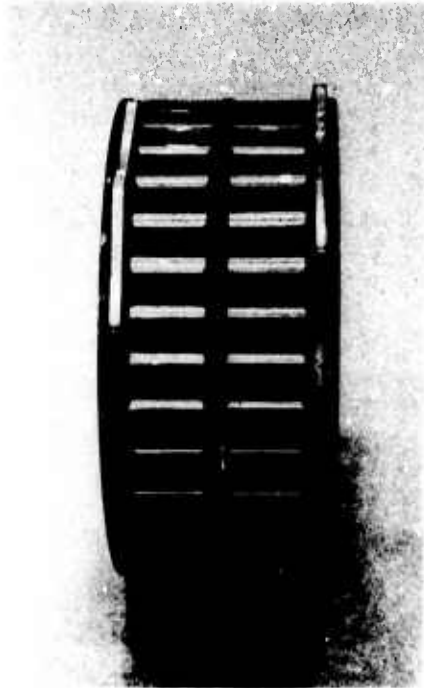


Figure 5. Design B--Borg-Warner X137675.

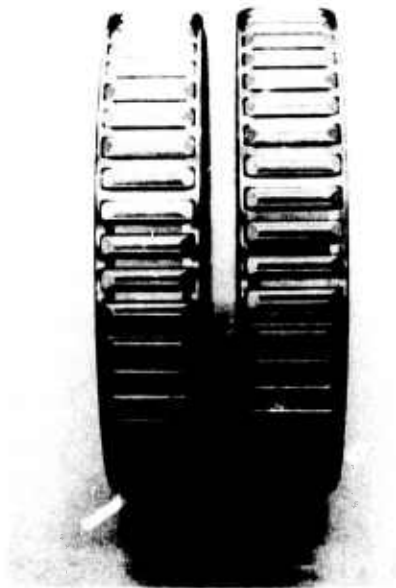
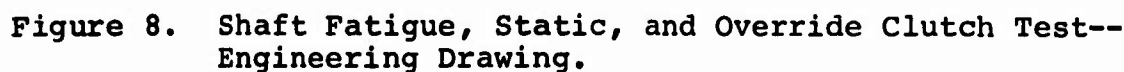
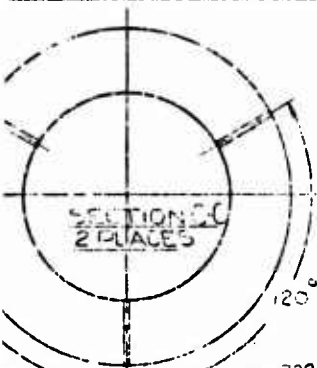


Figure 6. Design C--Formsprag CL-41802.



Figure 7. Optimized Design D--Borg-Warner X137920.

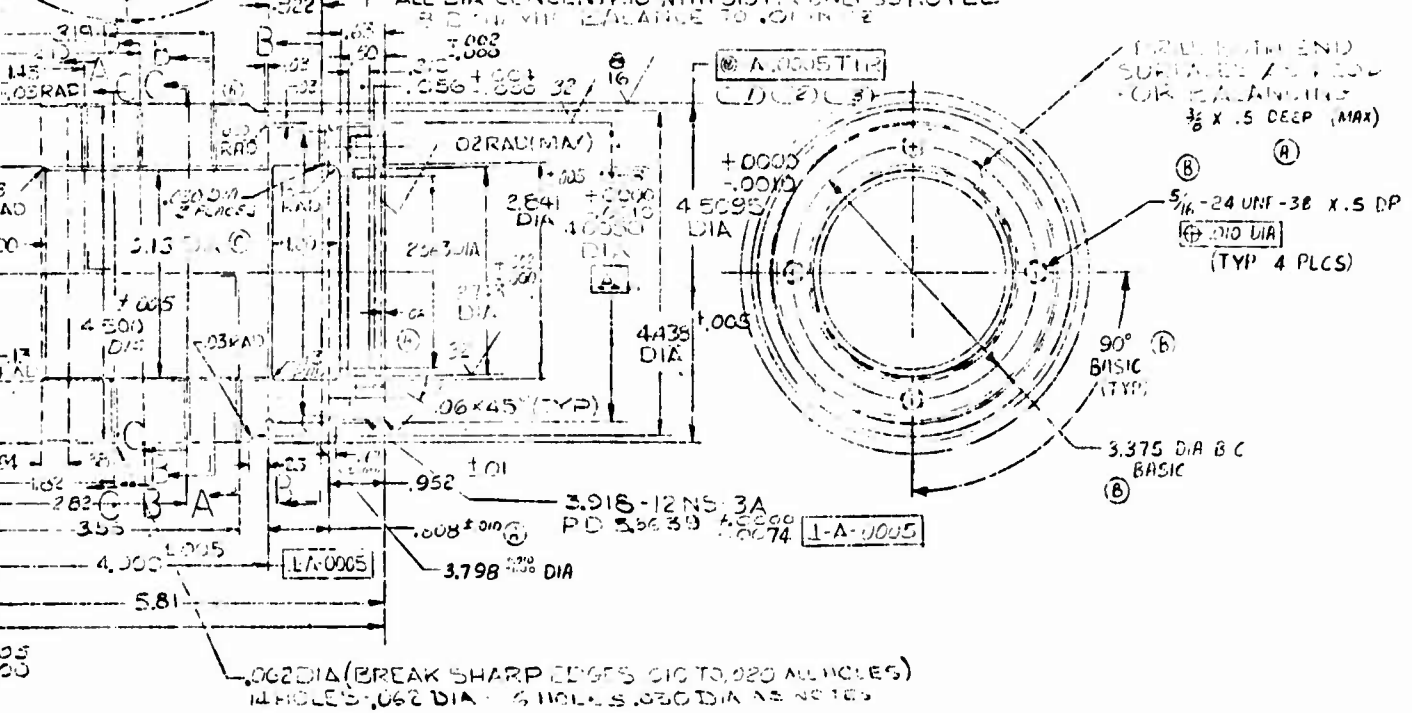




NOTES

- (1) MAX TAPER PERMITTED OVER LENGTH OF THIS DIA IS .0002 STEPS. THIS DIA ARE NOT PERMITTED
- (2) DO NOT SLACK OXIDE THIS DIA
- (3) HEAT TREAT PER BOEING DOCUMENT D210-10342-1
ACARBURIZED CASE HARDNESS
ROCKWELL C60-64
EFFECTIVE CASE DEPTH AFTER GRINDING .070-1.10
C-CORE HARDNESS ROCKWELL C36-42
- (4) MAT'L-STEEL PER BOEING SPEC X8MS 4223
- (5) MAX FINISH UNLESS NOTED
- (7) ALL DIA CONCENTRIC WITH CENTER UNLESS NOTED

REVISIONS			
REV	DATE	DESCRIPTION	DATE APPROVED
1	1/13	CHANGED DIA 1.000 TO 1.000	
2	1/13	CHANGED DIA 1.000 TO 1.000	
3	1/13	CHANGED DIA 1.000 TO 1.000	
4	1/13	CHANGED DIA 1.000 TO 1.000	



AMR 40872-1			
PART OR IDENTIFYING NUMBER			
MATERIAL & SPECIFICATION			
LIST OF MATERIAL			
THE B & W COMPANY			
VICTOR DIVISION PHILADELPHIA, PA			
40872-1			

atch Test--

B

7 DYNAMIC BALANCE TO .01 IN OZ

awing.

REV	DATE	BY	CHKD	DESCRIPTION
1	10-10-69	DCN		DESIGN
2	10-10-69	DCN		DESIGN
3	10-10-69	DCN		DESIGN
4	10-10-69	DCN		DESIGN
5	10-10-69	DCN		DESIGN
6	10-10-69	DCN		DESIGN
7	10-10-69	DCN		DESIGN
8	10-10-69	DCN		DESIGN
9	10-10-69	DCN		DESIGN
10	10-10-69	DCN		DESIGN
11	10-10-69	DCN		DESIGN
12	10-10-69	DCN		DESIGN
13	10-10-69	DCN		DESIGN
14	10-10-69	DCN		DESIGN
15	10-10-69	DCN		DESIGN
16	10-10-69	DCN		DESIGN
17	10-10-69	DCN		DESIGN
18	10-10-69	DCN		DESIGN
19	10-10-69	DCN		DESIGN
20	10-10-69	DCN		DESIGN
21	10-10-69	DCN		DESIGN
22	10-10-69	DCN		DESIGN
23	10-10-69	DCN		DESIGN
24	10-10-69	DCN		DESIGN
25	10-10-69	DCN		DESIGN
26	10-10-69	DCN		DESIGN
27	10-10-69	DCN		DESIGN
28	10-10-69	DCN		DESIGN
29	10-10-69	DCN		DESIGN
30	10-10-69	DCN		DESIGN
31	10-10-69	DCN		DESIGN
32	10-10-69	DCN		DESIGN
33	10-10-69	DCN		DESIGN
34	10-10-69	DCN		DESIGN
35	10-10-69	DCN		DESIGN
36	10-10-69	DCN		DESIGN
37	10-10-69	DCN		DESIGN
38	10-10-69	DCN		DESIGN
39	10-10-69	DCN		DESIGN
40	10-10-69	DCN		DESIGN
41	10-10-69	DCN		DESIGN
42	10-10-69	DCN		DESIGN
43	10-10-69	DCN		DESIGN
44	10-10-69	DCN		DESIGN
45	10-10-69	DCN		DESIGN
46	10-10-69	DCN		DESIGN
47	10-10-69	DCN		DESIGN
48	10-10-69	DCN		DESIGN
49	10-10-69	DCN		DESIGN
50	10-10-69	DCN		DESIGN
51	10-10-69	DCN		DESIGN
52	10-10-69	DCN		DESIGN
53	10-10-69	DCN		DESIGN
54	10-10-69	DCN		DESIGN
55	10-10-69	DCN		DESIGN
56	10-10-69	DCN		DESIGN
57	10-10-69	DCN		DESIGN
58	10-10-69	DCN		DESIGN
59	10-10-69	DCN		DESIGN
60	10-10-69	DCN		DESIGN
61	10-10-69	DCN		DESIGN
62	10-10-69	DCN		DESIGN
63	10-10-69	DCN		DESIGN
64	10-10-69	DCN		DESIGN
65	10-10-69	DCN		DESIGN
66	10-10-69	DCN		DESIGN
67	10-10-69	DCN		DESIGN
68	10-10-69	DCN		DESIGN
69	10-10-69	DCN		DESIGN
70	10-10-69	DCN		DESIGN
71	10-10-69	DCN		DESIGN
72	10-10-69	DCN		DESIGN
73	10-10-69	DCN		DESIGN
74	10-10-69	DCN		DESIGN
75	10-10-69	DCN		DESIGN
76	10-10-69	DCN		DESIGN
77	10-10-69	DCN		DESIGN
78	10-10-69	DCN		DESIGN
79	10-10-69	DCN		DESIGN
80	10-10-69	DCN		DESIGN
81	10-10-69	DCN		DESIGN
82	10-10-69	DCN		DESIGN
83	10-10-69	DCN		DESIGN
84	10-10-69	DCN		DESIGN
85	10-10-69	DCN		DESIGN
86	10-10-69	DCN		DESIGN
87	10-10-69	DCN		DESIGN
88	10-10-69	DCN		DESIGN
89	10-10-69	DCN		DESIGN
90	10-10-69	DCN		DESIGN
91	10-10-69	DCN		DESIGN
92	10-10-69	DCN		DESIGN
93	10-10-69	DCN		DESIGN
94	10-10-69	DCN		DESIGN
95	10-10-69	DCN		DESIGN
96	10-10-69	DCN		DESIGN
97	10-10-69	DCN		DESIGN
98	10-10-69	DCN		DESIGN
99	10-10-69	DCN		DESIGN
100	10-10-69	DCN		DESIGN

REV	DATE	BY	CHKD	DESCRIPTION
1	10-10-69	DCN		DESIGN
2	10-10-69	DCN		DESIGN
3	10-10-69	DCN		DESIGN
4	10-10-69	DCN		DESIGN
5	10-10-69	DCN		DESIGN
6	10-10-69	DCN		DESIGN
7	10-10-69	DCN		DESIGN
8	10-10-69	DCN		DESIGN
9	10-10-69	DCN		DESIGN
10	10-10-69	DCN		DESIGN
11	10-10-69	DCN		DESIGN
12	10-10-69	DCN		DESIGN
13	10-10-69	DCN		DESIGN
14	10-10-69	DCN		DESIGN
15	10-10-69	DCN		DESIGN
16	10-10-69	DCN		DESIGN
17	10-10-69	DCN		DESIGN
18	10-10-69	DCN		DESIGN
19	10-10-69	DCN		DESIGN
20	10-10-69	DCN		DESIGN
21	10-10-69	DCN		DESIGN
22	10-10-69	DCN		DESIGN
23	10-10-69	DCN		DESIGN
24	10-10-69	DCN		DESIGN
25	10-10-69	DCN		DESIGN
26	10-10-69	DCN		DESIGN
27	10-10-69	DCN		DESIGN
28	10-10-69	DCN		DESIGN
29	10-10-69	DCN		DESIGN
30	10-10-69	DCN		DESIGN
31	10-10-69	DCN		DESIGN
32	10-10-69	DCN		DESIGN
33	10-10-69	DCN		DESIGN
34	10-10-69	DCN		DESIGN
35	10-10-69	DCN		DESIGN
36	10-10-69	DCN		DESIGN
37	10-10-69	DCN		DESIGN
38	10-10-69	DCN		DESIGN
39	10-10-69	DCN		DESIGN
40	10-10-69	DCN		DESIGN
41	10-10-69	DCN		DESIGN
42	10-10-69	DCN		DESIGN
43	10-10-69	DCN		DESIGN
44	10-10-69	DCN		DESIGN
45	10-10-69	DCN		DESIGN
46	10-10-69	DCN		DESIGN
47	10-10-69	DCN		DESIGN
48	10-10-69	DCN		DESIGN
49	10-10-69	DCN		DESIGN
50	10-10-69	DCN		DESIGN
51	10-10-69	DCN		DESIGN
52	10-10-69	DCN		DESIGN
53	10-10-69	DCN		DESIGN
54	10-10-69	DCN		DESIGN
55	10-10-69	DCN		DESIGN
56	10-10-69	DCN		DESIGN
57	10-10-69	DCN		DESIGN
58	10-10-69	DCN		DESIGN
59	10-10-69	DCN		DESIGN
60	10-10-69	DCN		DESIGN
61	10-10-69	DCN		DESIGN
62	10-10-69	DCN		DESIGN
63	10-10-69	DCN		DESIGN
64	10-10-69	DCN		DESIGN
65	10-10-69	DCN		DESIGN
66	10-10-69	DCN		DESIGN
67	10-10-69	DCN		DESIGN
68	10-10-69	DCN		DESIGN
69	10-10-69	DCN		DESIGN
70	10-10-69	DCN		DESIGN
71	10-10-69	DCN		DESIGN
72	10-10-69	DCN		DESIGN
73	10-10-69	DCN		DESIGN
74	10-10-69	DCN		DESIGN
75	10-10-69	DCN		DESIGN
76	10-10-69	DCN		DESIGN
77	10-10-69	DCN		DESIGN
78	10-10-69	DCN		DESIGN
79	10-10-69	DCN		DESIGN
80	10-10-69	DCN		DESIGN
81	10-10-69	DCN		DESIGN
82	10-10-69	DCN		DESIGN
83	10-10-69	DCN		DESIGN
84	10-10-69	DCN		DESIGN
85	10-10-69	DCN		DESIGN
86	10-10-69	DCN		DESIGN
87	10-10-69	DCN		DESIGN
88	10-10-69	DCN		DESIGN
89	10-10-69	DCN		DESIGN
90	10-10-69	DCN		DESIGN
91	10-10-69	DCN		DESIGN
92	10-10-69	DCN		DESIGN
93	10-10-69	DCN		DESIGN
94	10-10-69	DCN		DESIGN
95	10-10-69	DCN		DESIGN
96	10-10-69	DCN		DESIGN
97	10-10-69	DCN		DESIGN
98	10-10-69	DCN		DESIGN
99	10-10-69	DCN		DESIGN
100	10-10-69	DCN		DESIGN

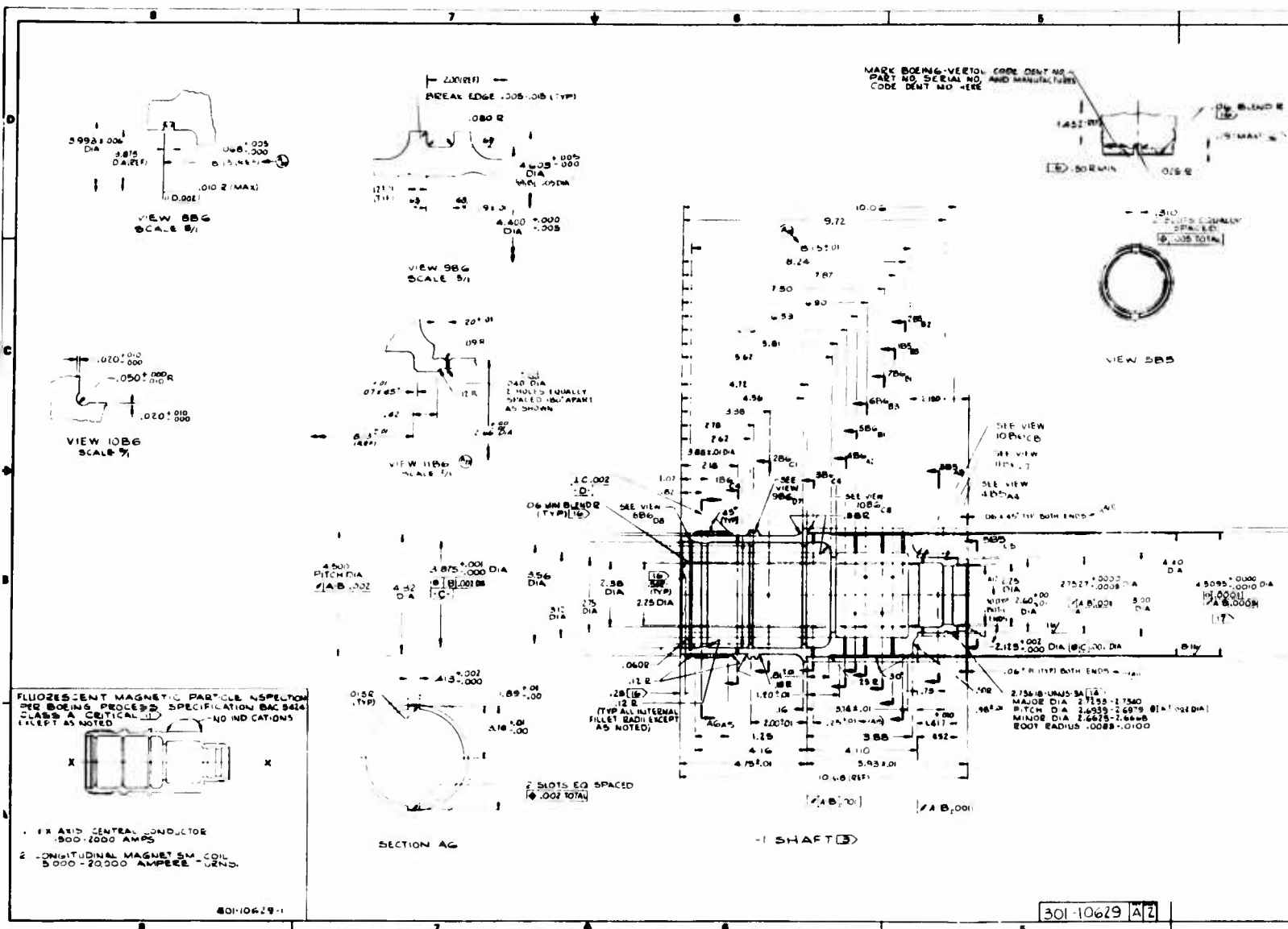
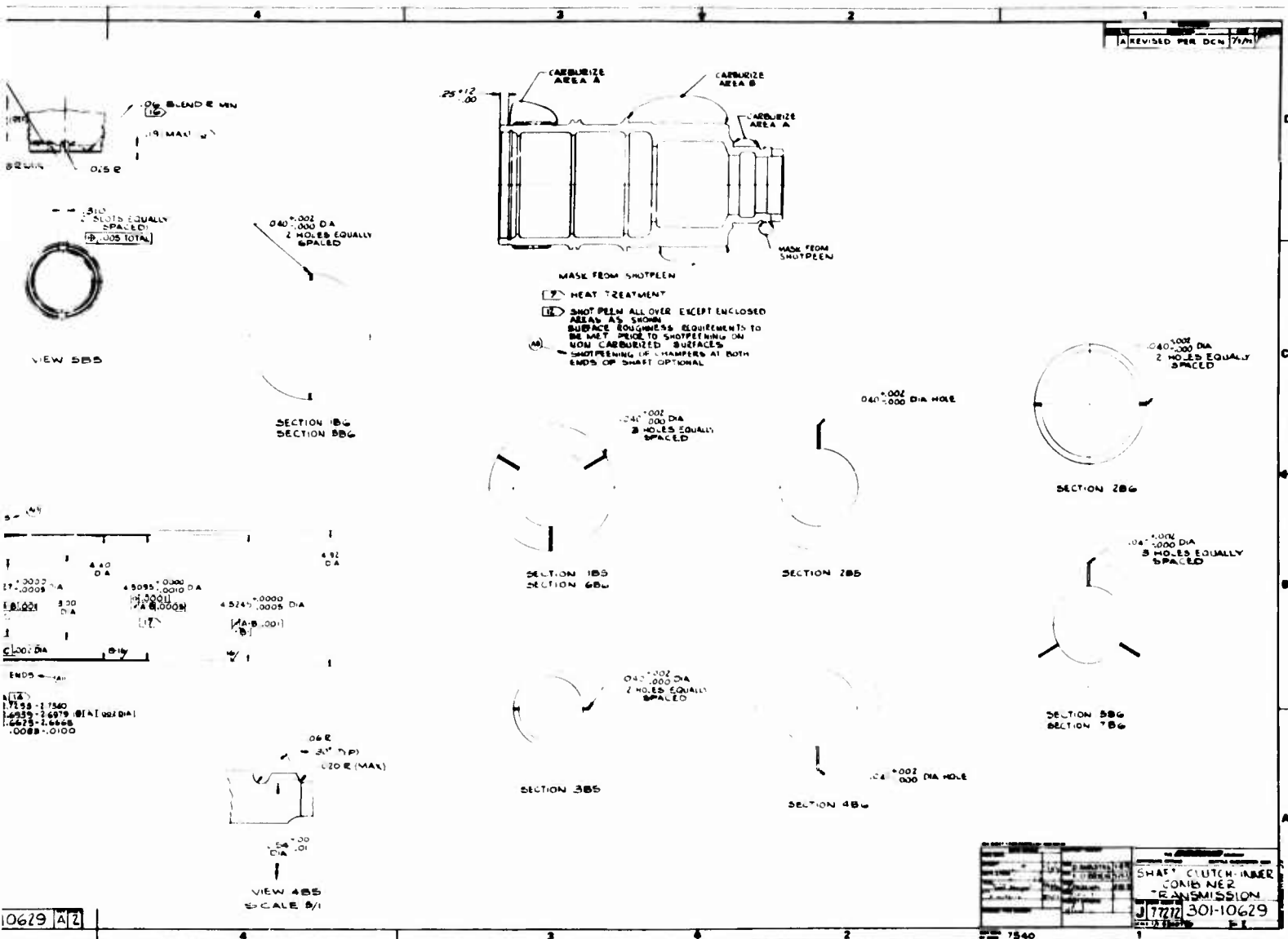


Figure 10. Inner Clutch Shaft of Combiner Transmission--
Engineering Drawing (Sheet 1 of 2).

Preceding page blank

ITEM	REV	DESCRIPTION	DATE	BY	CHKD
(11)	00	ADDED LUMBER DEPTH, 0.5" (TYP) BOTH ENDS	10-1-62	J. A. C.	
(12)	00	ADDED LUMBER DEPTH, 3" (TYP) BOTH ENDS	10-1-62	J. A. C.	
(13)	00	ADDED RADIUS LUMBER, 0.625" (TYP) BOTH ENDS	10-1-62	J. A. C.	
(14)	00	1.67 IN. WAS 1.5 IN.	10-1-62	J. A. C.	
(15)	00	ADDED .25 IN.	10-1-62	J. A. C.	
(16)	00	ADDED LUMBER, 3" (TYP) BOTH ENDS	10-1-62	J. A. C.	
(17)	00	ADDED 2 IN.	10-1-62	J. A. C.	
(18)	00	ADDED 0.125 IN.	10-1-62	J. A. C.	
(19)	00	.07 WAS .05	10-1-62	J. A. C.	
(20)	00	.02 WAS .01	10-1-62	J. A. C.	
(21)	00	ADDED .002 IN.	10-1-62	J. A. C.	
(22)	00	ADDED .002 IN.	10-1-62	J. A. C.	
(23)	00	ADDED .002 IN.	10-1-62	J. A. C.	
(24)	00	ADDED .002 IN.	10-1-62	J. A. C.	
(25)	00	ADDED .002 IN.	10-1-62	J. A. C.	
(26)	00	ADDED .002 IN.	10-1-62	J. A. C.	
(27)	00	ADDED .002 IN.	10-1-62	J. A. C.	
(28)	00	ADDED .002 IN.	10-1-62	J. A. C.	
(29)	00	ADDED .002 IN.	10-1-62	J. A. C.	
(30)	00	ADDED .002 IN.	10-1-62	J. A. C.	

ITEM	REV	DESCRIPTION	DATE	BY	CHKD
(10)	00	ADDED .002 IN. TO SHAFT DEPTH (DIMENSIONED)	10-1-62	J. A. C.	
(11)	00	ADDED .002 IN. TO SHAFT DEPTH (DIMENSIONED)	10-1-62	J. A. C.	
(12)	00	ADDED .002 IN. TO SHAFT DEPTH (DIMENSIONED)	10-1-62	J. A. C.	
(13)	00	ADDED .002 IN. TO SHAFT DEPTH (DIMENSIONED)	10-1-62	J. A. C.	
(14)	00	ADDED .002 IN. TO SHAFT DEPTH (DIMENSIONED)	10-1-62	J. A. C.	
(15)	00	ADDED .002 IN. TO SHAFT DEPTH (DIMENSIONED)	10-1-62	J. A. C.	
(16)	00	ADDED .002 IN. TO SHAFT DEPTH (DIMENSIONED)	10-1-62	J. A. C.	
(17)	00	ADDED .002 IN. TO SHAFT DEPTH (DIMENSIONED)	10-1-62	J. A. C.	
(18)	00	ADDED .002 IN. TO SHAFT DEPTH (DIMENSIONED)	10-1-62	J. A. C.	
(19)	00	ADDED .002 IN. TO SHAFT DEPTH (DIMENSIONED)	10-1-62	J. A. C.	
(20)	00	ADDED .002 IN. TO SHAFT DEPTH (DIMENSIONED)	10-1-62	J. A. C.	
(21)	00	ADDED .002 IN. TO SHAFT DEPTH (DIMENSIONED)	10-1-62	J. A. C.	
(22)	00	ADDED .002 IN. TO SHAFT DEPTH (DIMENSIONED)	10-1-62	J. A. C.	
(23)	00	ADDED .002 IN. TO SHAFT DEPTH (DIMENSIONED)	10-1-62	J. A. C.	
(24)	00	ADDED .002 IN. TO SHAFT DEPTH (DIMENSIONED)	10-1-62	J. A. C.	
(25)	00	ADDED .002 IN. TO SHAFT DEPTH (DIMENSIONED)	10-1-62	J. A. C.	
(26)	00	ADDED .002 IN. TO SHAFT DEPTH (DIMENSIONED)	10-1-62	J. A. C.	
(27)	00	ADDED .002 IN. TO SHAFT DEPTH (DIMENSIONED)	10-1-62	J. A. C.	
(28)	00	ADDED .002 IN. TO SHAFT DEPTH (DIMENSIONED)	10-1-62	J. A. C.	
(29)	00	ADDED .002 IN. TO SHAFT DEPTH (DIMENSIONED)	10-1-62	J. A. C.	
(30)	00	ADDED .002 IN. TO SHAFT DEPTH (DIMENSIONED)	10-1-62	J. A. C.	



10629 A2

SHAFT CLUTCH INNER CONE NUT TRANSMISSION	J 7772 301-10629
--	------------------

Figure 10. Continued (Sheet 2 of 2).

DESIGN REQUIREMENTS

SPECIFICATIONS:

- A) RATED TORQUE 7500 FT LBS
- B) NUMBER OF SPRAGS 68 (34/ROW)
- C) DRAG-OUTER CAGE 800-800 IN OZ
- D) DRAG-ASSEMBLY 150-150 IN OZ
- E) DRAG BANDS 2
- F) CLUTCH MUST HOLD TO OUTER RACE
- G) GROUP SPRAGS WITHIN .0003 AT 15° RELEASE AND .0006 AT 15° LOCK DIMENSIONS FOR EACH ASSEMBLY.

DESIGN REQUIREMENTS

SPECIFICATIONS:

- A) RATED TORQUE 7500 FT LBS
- B) NUMBER OF SPRAGS 68 (34/ROW)
- C) DRAG-OUTER CAGE 800-800 IN OZ
- D) DRAG-ASSEMBLY 150-150 IN OZ
- E) DRAG STRIPS 2
- F) DRAG BANDS 2
- G) CLUTCH MUST HOLD TO OUTER RACE
- H) GROUP SPRAGS WITHIN .0003 AT 15° RELEASE AND .0006 AT 15° LOCK DIMENSIONS FOR EACH ASSEMBLY

MARK BOEING VERTOL PART NO. & CODE IDENT NO. VENDOR PART NO. & CODE IDENT NO. HERE. CODE IDENT NOS. TO BE IN PARENTHESES.

MARK BOEING VERTOL PART NO. & CODE IDENT NO. VENDOR PART NO. & CODE IDENT NO. HERE. CODE IDENT NOS. TO BE IN PARENTHESES.

*5085 *5085 INNER RACE O.D. (REF)

FREE WHEEL DIRECTION OF INNER RACE



*5085 *5085 OUTER RACE I.D. (REF)



*5085 *5085 INNER RACE O.D. (REF)

FREE WHEEL DIRECTION OF INNER RACE



*5085 *5085 OUTER RACE I.D. (REF)



*5085 *5085 OUTER RACE I.D. (REF)

-2
SAME AS 1 EXCEPT AS SHOWN

301-10646 7

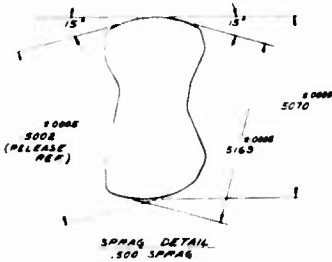
Figure 11. Engine Clutch Shaft of Combiner Transmission--
Engineering Drawing.

Preceding page blank

NOTES CONT

- 1. MATERIAL:**
A. CAGES - 6340 STEEL WITH NITRIDED SURFACES
B. SPRAGS - M50 STEEL, HARDENED TO Rc 61-65, NO DECARB OR RETAINED AUSTENITE PERMISSIBLE
C. DRAG STRIPS - NO 25 BERYLCO WITH .008 SILVER PLATING
D. DRAG BANDS - NO 25 BERYLCO
- 2. DRAG STRIPS, BANDS AND RIBBON TO BE 100% FLUORESCENT PENETRANT INSPECTED PER BOEING PROCESS SPECIFICATION DAC 5423 ACCEPTANCE CRITERIA - NO INDICATIONS ALLOWED**
- 3. CAGES SHALL BE 100% FLUORESCENT PENETRANT INSPECTED PER BOEING PROCESS SPECIFICATION DAC 5423 ACCEPTANCE CRITERIA - NO INDICATION ALLOWED**
- 4. SPRAGS SHALL BE 100% FLUORESCENT MAGNETIC PARTICLE INSPECTED PER BOEING PROCESS SPECIFICATION DAC 5424 ACCEPTANCE CRITERIA - NO INDICATION ALLOWED**
- 5. SPRAGS SHALL BE COLOR CODED IN RED, BLUE, YELLOW AND GREEN BY THE MANUFACTURER TO DENOTE SIZE GROUPINGS. ONLY SPRAGS OF ONE COLOR ARE PERMITTED IN A CLUTCH ASSY. THE COLORED PORTION OF EACH SPRAG MUST BE ORIENTED IN THE SAME WAY**
COLOR CODE AND SIZE SHOWN BELOW:
RED - 4996 - 4999
BLUE - 4999 - 5002
YELLOW - 5002 - 5005
GREEN - 5005 - 5008

- 1. MATERIAL:**
A. CAGES - 6340 STEEL WITH NITRIDED SURFACES
B. SPRAGS - M50 STEEL, HARDENED TO Rc 61-65, MICROSCOPIC EXAMINATION (SOC+) SHALL REVEAL NO VISUAL RETAINED AUSTENITE OR DECARB AFTER ETCHING IN 2% NITRIC ACID AND ALCOHOL
C. DRAG BANDS - NO 25 BERYLCO



APPROVED SOURCES OF SUPPLY			
BOEING PART NO.	SUPPLIER NAME ADDRESS	SUPPLIER PART NO.	SUPPLIER CAGE NO.
1	2 5008 (GEM)		
2			

2 5008 (GEM)			
1 5008 (GEM)			

- 1. UNLESS OTHERWISE SPECIFIED, ALL DIMENSIONS ARE IN INCHES.**
2. ONLY THE ITEMS DESCRIBED ON THIS DRAWING WHEN PROCURED FROM THE VENDOR(S) LISTED HEREON IS APPROVED BY BOEING-VERTEL DIVISION, PHILA, PENNA. FOR USE IN THE APPLICATION(S) SPECIFIED HEREON. A SUBSTITUTE ITEM SHALL NOT BE USED WITHOUT PRIOR TESTING AND APPROVAL BY BOEING-VERTEL DIVISION, PHILA, PENNA. OR BY THE U.S. ARMY AVIATION SYSTEMS COMMAND, ST LOUIS, MO
3. THIS DRAWING SHOWS THE MINIMUM INSPECTION REQUIRED ON THE VENDOR DRAWING. BASIC DIMENSIONAL REQUIREMENTS COMMON TO ALL VENDORS APPEAR ON THIS DRAWING.
4. SUPPLIER SHALL CONFORM TO ALL REQUIREMENTS OF DSOI-10646-1.
5. CLUTCH ASSEMBLY SHALL BE INDIVIDUALLY BAGGED OR CONTAINERIZED WITH THE BOEING VERTOL PART NUMBER, LODS IDENT NO, MANUFACTURE CODE IDENT NO, PART NO AND SERIAL NO. RUBBER STAMPED ON THE PACKAGE PER DAC 5807 TYPE RS

SOURCE CONTROL DRAWING

301-10646-1	CLUTCH ASSY	VE
301-10646-1	CLUTCH ASSY	VE

301-10646-1	CLUTCH ASSY	VE
301-10646-1	CLUTCH ASSY	VE

CLUTCH ASSEMBLY
 ENGINE SHAFT
 COMBINER TRANSMISSION
 J17272 301-10646

7540

TEST FACILITY

DYNAMIC TESTS

Test Stand

The test stand shown in Figures 13 and 14 consisted of two independently controlled speed increasers mounted on a solid weldment. The output shafts of the speed increasers were aligned to within 0.010 inch total indicated reading, and the specimen mounting-pad parallelism was maintained within 0.010 inch. The specimen output shaft (clutch inner race) was controlled by a variable-speed 60-hp dc motor driving through an overall ratio of 4.3125:1. The input shaft (clutch outer race) was controlled by a 70-hp hydraulic motor, powered by a 100-hp pump, driving through a ratio of 7.59:1. The test-stand gearboxes were lubricated by a system totally independent of the test-specimen lubrication system, as shown in Figure 15. The cartridge containing the test clutch could be installed between the two speed increasers without moving either gearbox, which provided for rapid removal and ensured constant proper alignment. The test specimen was lubricated by an independent lubrication system using MIL-L-23699 oil. An immersion heater maintained a constant oil-in temperature of 200°F. Hot oil exited from the specimen cartridge by gravity flow only.

Instrumentation

The instrumentation package consisted of constant-view monitoring devices. The monitored data included:

- Oil flow to specimen
- Oil flow to test-stand gearboxes
- Oil pressure to specimen
- Oil pressure to specimen-support bearings
- Oil pressure to test-stand gearboxes
- Oil temperature to specimen
- Oil temperature from specimen
- Oil temperature from specimen-support bearings
- Clutch drag torque
- Clutch inner-race speed
- Clutch outer-race speed
- Test-stand gearbox input speed
- Drive-motor speed
- Drive-motor amperage

Oil temperatures were measured using iron-constantan thermocouples in the scavenge lines.

Torque was measured using a strain-gauged necked-down shaft

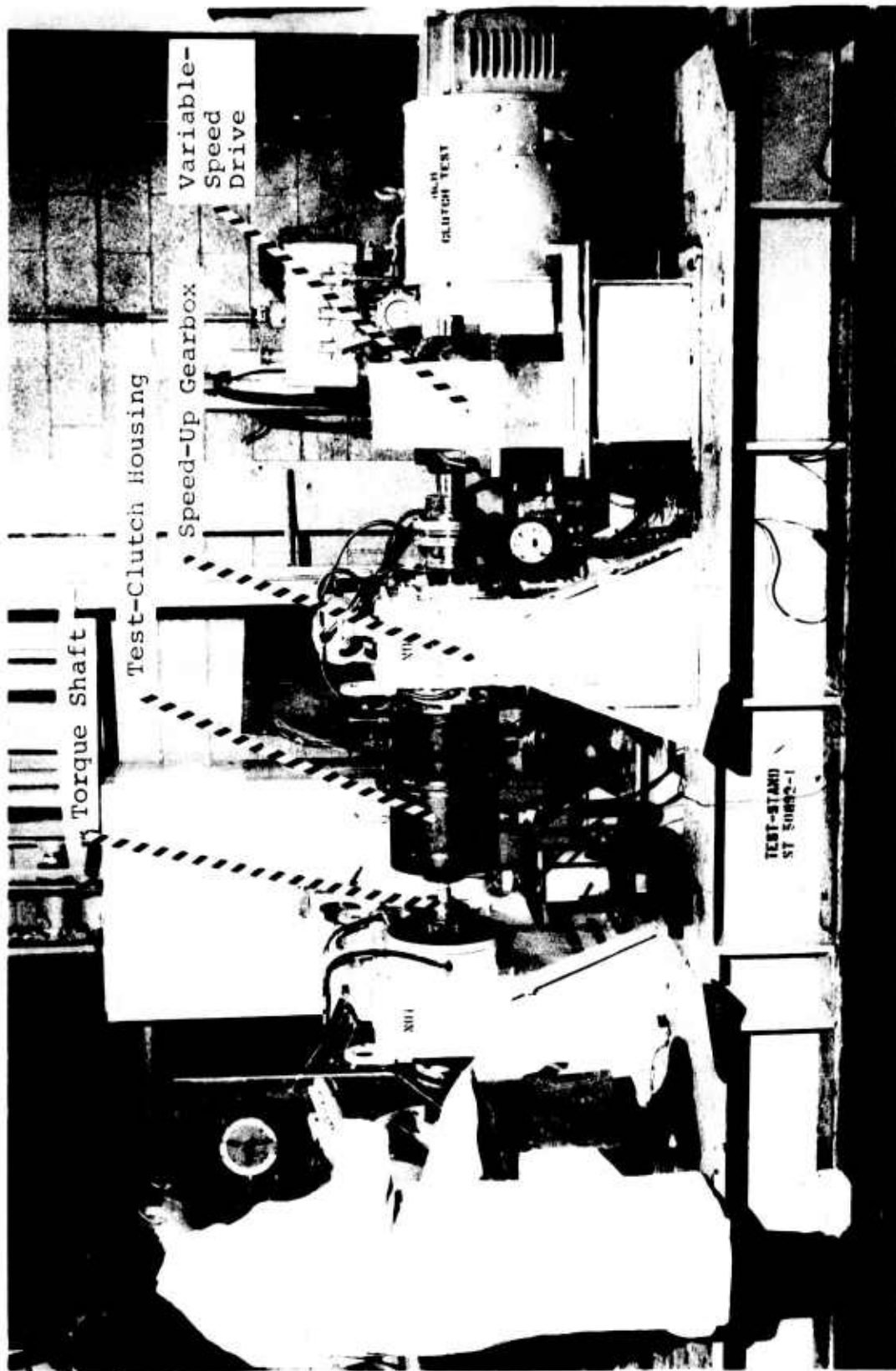


Figure 13. Dynamic Clutch-Test Facility.

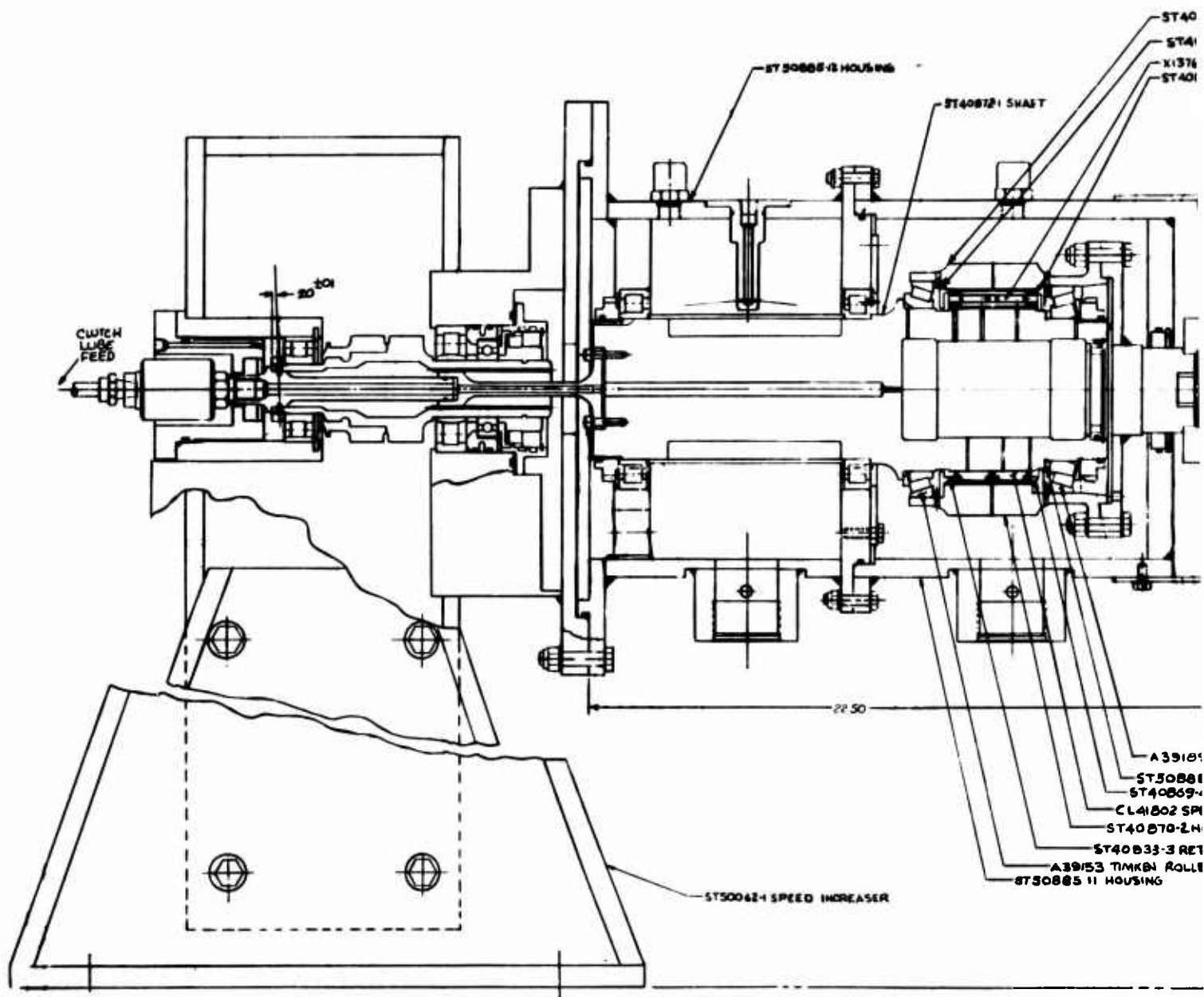
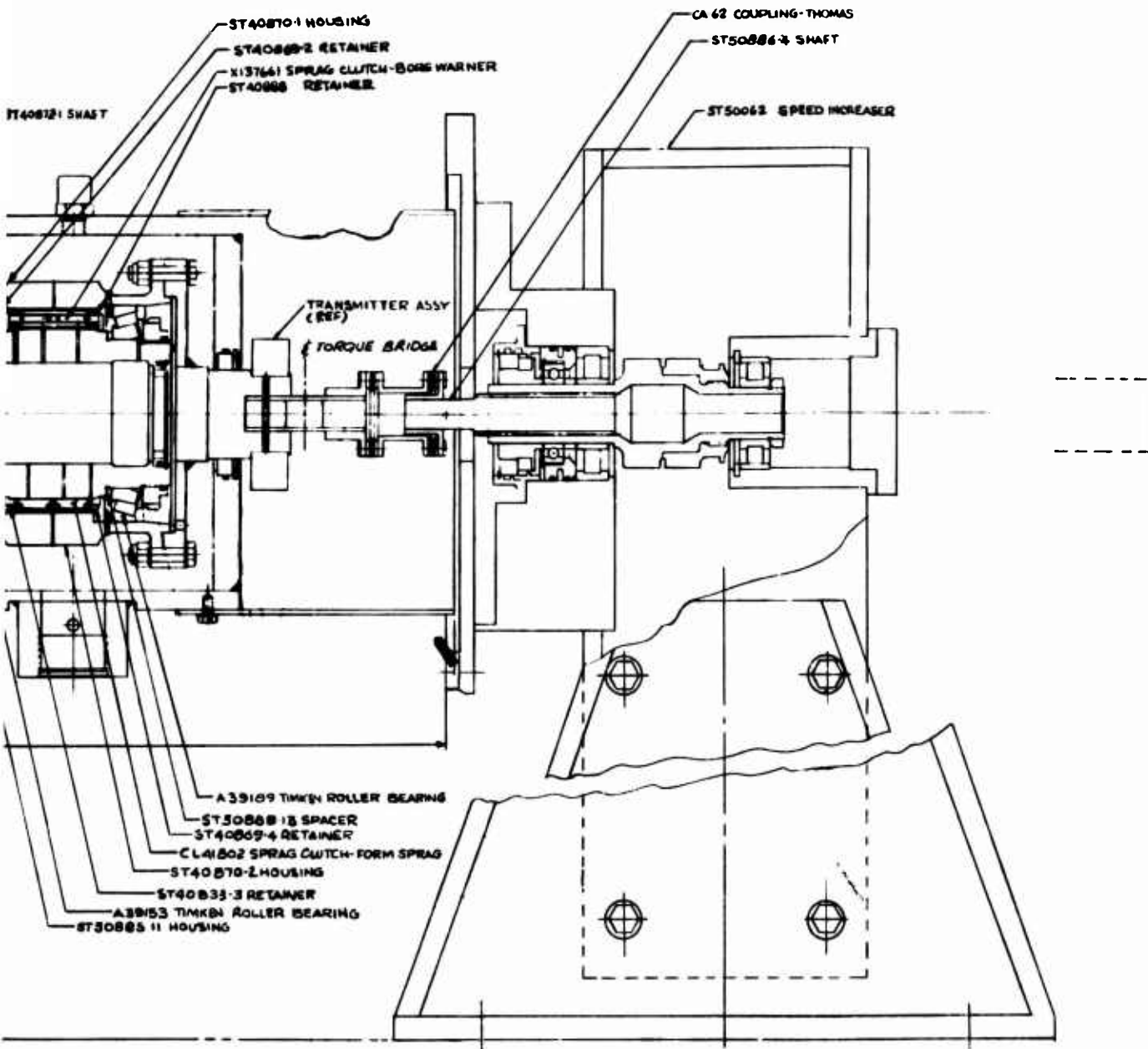


Figure 14. Clutch-Test Fixture Variable-Speed Overrun Subassembly.

Preceding page blank



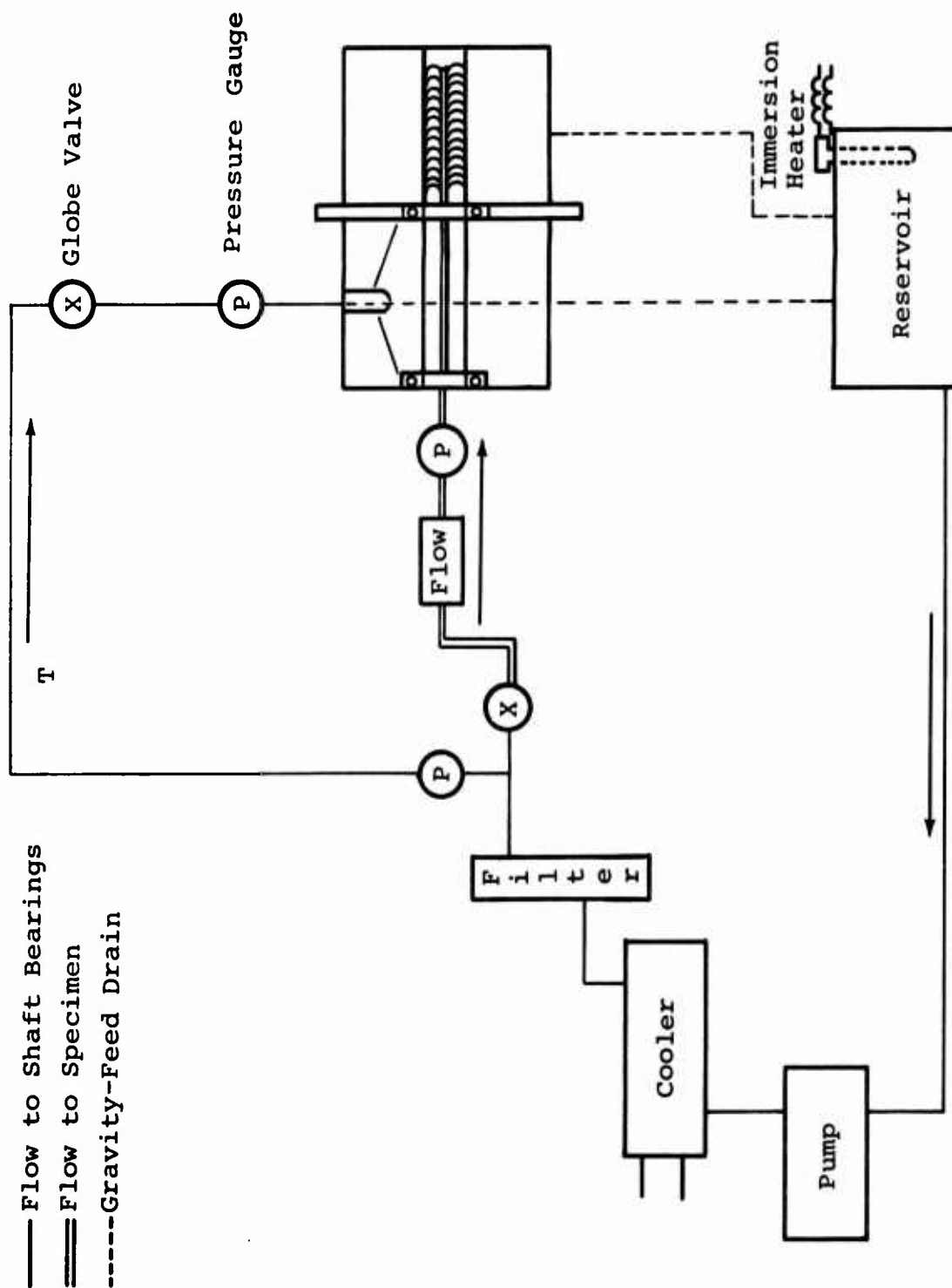


Figure 15. Clutch-Test Lubrication System.

attached to the clutch outer race. The torque was transmitted through an Acurex telemetry system and displayed on a digital voltmeter. This system is shown in Figures 16 and 17.

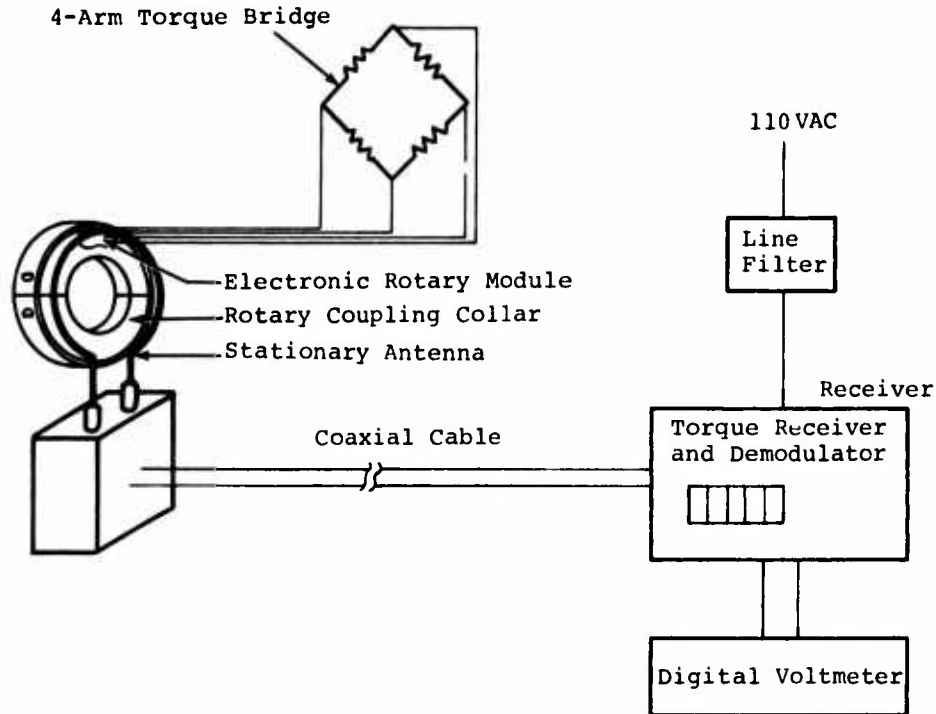


Figure 16. Acurex 1206 Telemetric Drag-Torque Readout System.

STATIC TEST

Fatigue and static torsional loadings of the clutch were applied by a hydraulic rotary actuator with a stall torque of 228,000 in.-lb at 3,000 psi. Maximum rotation was 100 degrees, controlled by a limit switch which actuated a servovalve that dumped the load. Figures 18 and 19 show this test setup.

The actuator was controlled by an electronic closed-loop servocontrol system. Feedback to the servosystem was supplied from a strain-gauge torsion bridge through a torque transducer. The reacted torque from the clutch was measured by a second strain-gauge torque bridge. Before testing, both bridges were calibrated to 120,000 in.-lb. Steady torque levels for both the fatigue and static-overload tests were applied by the positioning of the servocontroller set-point knob. The set-point position was determined from the torque-transducer output. The alternating fatigue load about the steady load was applied by another control knob on the servocontroller. Measurements of the dynamic fatigue loads were monitored on a recording oscillograph. Static-overload measurements were recorded on a strain indicator coupled to the torque transducer.

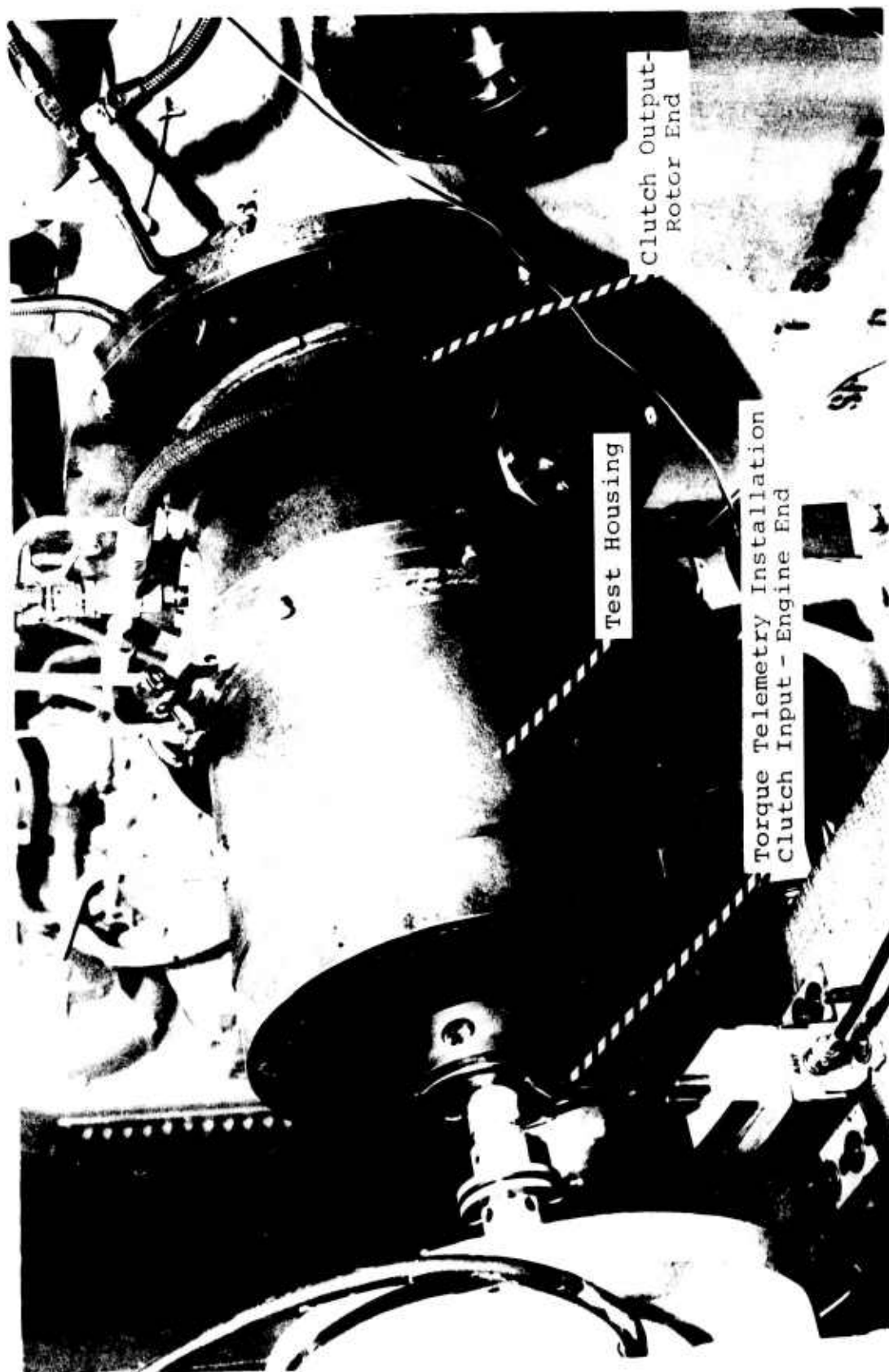
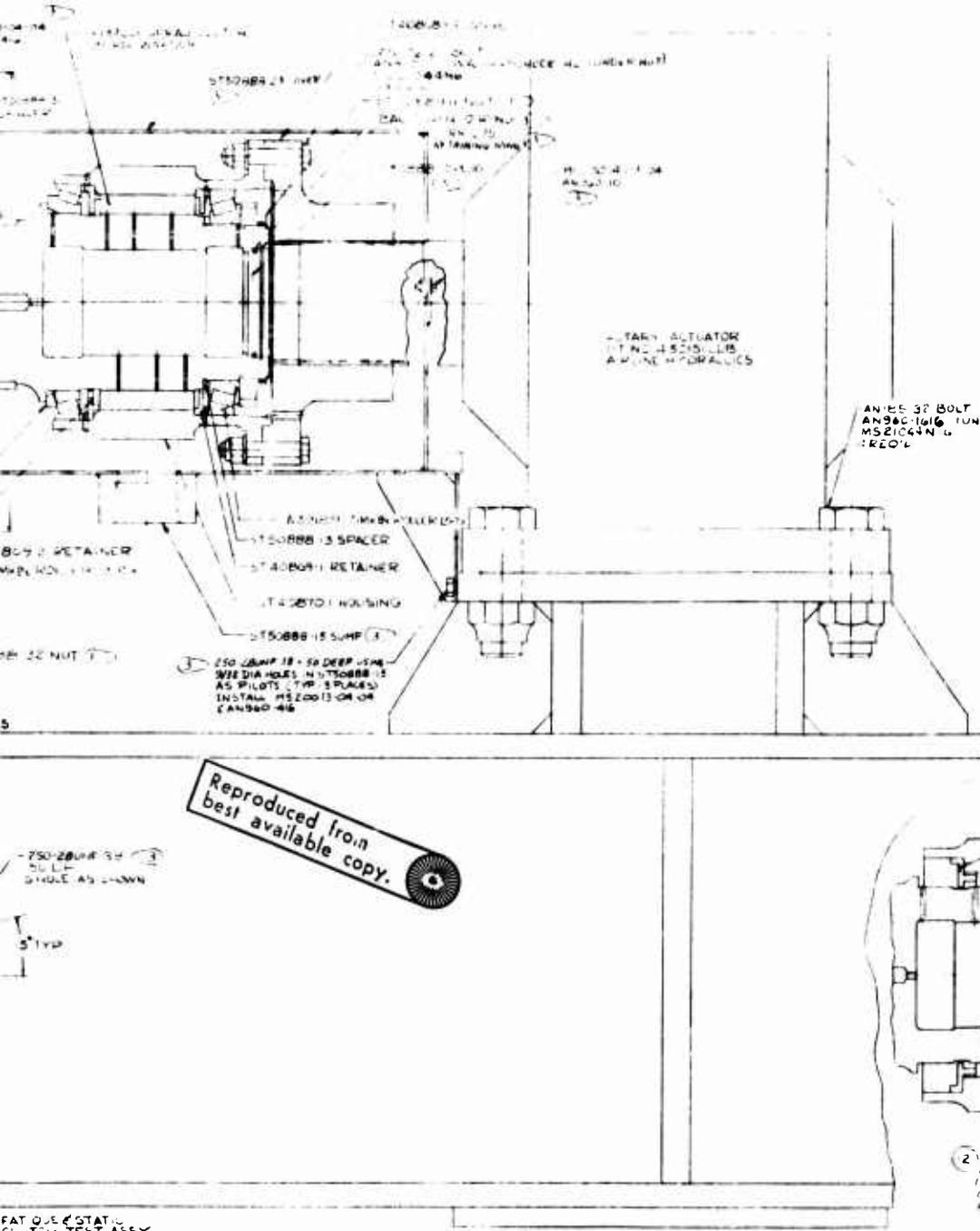


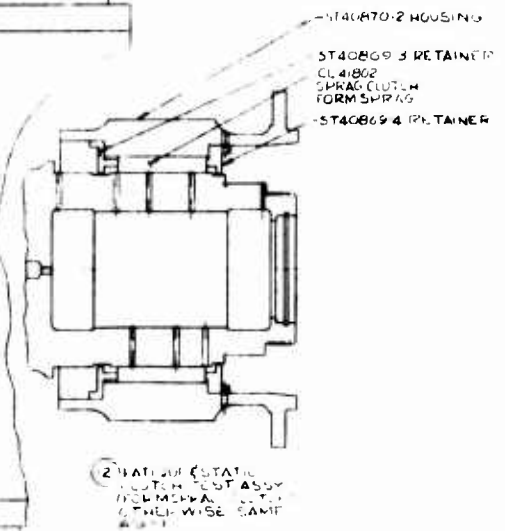
Figure 17. Dynamic Test-Specimen Cartridge and Acurex Telemetry System.



Fig. 18. Clutch Cyclic Torque Test.



NOTES
 (1) TORQUE TO 150 FT. LB.
 (2) HANDED PARTS WITH
 MOUNTING HOLES IN BASE
 (3) NOT REQD. REF ONLY



FAT OIL CLUTCH TEST ASSY (BORG WARNER)

TEST PROCEDURE

GENERAL

Six series of tests were conducted as follows:

- Full-speed overrun test
- Differential-speed overrun test
- Static overload test
- Nonrotating cyclic-torque slip test
- Static cyclic-torque fatigue test
- Differential-speed override 50-hour endurance test

Clutch Designs A, B, and C were subjected to the first two tests; Design D was subjected to all six tests.

MIL-L-233699 oil was used throughout all testing.

FULL-SPEED OVERRUN TEST

The objective of this test was to determine the optimum clutch oil flow in terms of heat generation, drag torque, and component wear. The following test data was monitored and recorded at half-hour intervals:

- Clutch-assembly oil temperature in °F, $\pm 2^{\circ}\text{F}$
- Clutch-assembly oil temperature out °F, $\pm 2^{\circ}\text{F}$
- Clutch-assembly oil flow gpm, ± 0.1 gpm
- Clutch-assembly oil pressure psi, actual
- Clutch drag torque in.-lb, ± 10 in.-lb
- Output-shaft speed rpm, ± 50 rpm
- Input-shaft speed rpm, ± 50 rpm
- Time of day hr min, actual
- Run time hr min, actual

All dynamic overrun testing was performed with the input shaft at zero speed and the output shaft running at 11,500 rpm. Four successive 5-hour tests were performed, as shown in Table I.

TABLE I. CONDITIONS FOR THE FULL-SPEED OVERRUN TEST			
Run	Oil Flow		
	(percentage of original design)	percentage of final design	(gpm)
1	300	150	6
2	200	100	4
3	100	50	2
4	67	33.5	1.3

The oil temperature into the clutch was maintained at 200°F, $\pm 2^\circ$, for all test runs. At the completion of each 5-hour run, the bearings, clutches, and inner and outer races were inspected for any discrepancies. One clutch of each Designs A, B, C, and D was subjected to the full-speed overrun test.

DIFFERENTIAL-SPEED OVERRUN TEST

The objective of this test was to determine the maximum heat rejection and drag condition resulting from the combination of rubbing speed and the effect of centrifugal force on the clutch sprags. The inner- and outer-race speeds were maintained as noted in Table II.

TABLE II. CONDITIONS FOR THE DIFFERENTIAL-SPEED OVERRUN TEST			
Run	Output-Shaft Speed (rpm)	Input-Shaft Speed (rpm)	Percentage of Normal Rate
1	11,500	5,750	50
2	11,500	7,705	67
3	11,500	8,625	75

During this test the oil flow for clutch Designs A, B, and C was maintained at 2 gpm, representing 100 percent of the original design oil flow to the clutch.

Because of marginal lubrication which occurred later during high-speed disengagement testing of Design B, the design oil flow was increased from the original design value of 2 gpm to a final design value of 4 gpm. Differential-speed overrun testing of the optimized Design D (an improvement on Design B) was accordingly conducted at 4 gpm except for the 50-hour differential-speed endurance test conducted on Design D. During this test, the oil flow was reduced to 3 gpm, representing 75 percent of the final aircraft transmission design oil flow, in order to determine if a margin of lubricity existed.

The same test data was monitored and recorded as in the full-speed overrun test at 15-minute intervals until the oil-in temperature stabilized at 200°F, $\pm 2^\circ$ F.

At the completion of each run, the clutch and clutch shafts were inspected for any discrepancies. The condition of the test specimens dictated if the succeeding test run was to be performed.

STATIC OVERLOAD TEST

The objective of this test was to determine the ultimate capacity of the clutch and the mode of an overload failure. This test was performed on the selected candidate clutch only, Design D, as selected from the results of the previous test.

Static torque was applied in the following increments:

- 250 ft-lb from 0 to 4,000 ft-lb
- 500 ft-lb from 4,000 to 8,000 ft-lb
- 2,000 ft-lb from 8,000 ft-lb to failure

The following test parameters were recorded at each torque setting:

- Torque ft-lb, ± 10 ft-lb
- Angular displacement degrees, ± 0.5 degrees
- Outer-shaft deflection over each
row of sprags--8 places inches, ± 0.0005 inch
- Load sharing between rows
of sprags percent, ± 20 percent

The clutch, inner and outer races, and bearings were coated with Mobil 28 (MIL-G-81322) grease.

The load distribution or sharing characteristics of the clutch was determined by machining a groove in the clutch inner race between the two rows of sprags and installing strain-gauge torque bridges. The gauges were then encapsulated in EC2216 epoxy. The load-sharing torsion bridges were calibrated in two steps. First, one row of sprags was removed from the clutch and 27,750 in.-lb of torque was applied in increments of 5,550 in.-lb. The second step was a repeat of the first step with only the second row of sprags installed. The interaction of compressive line contact strains with the torsion bridge was measured at 27,750 in.-lb.

NONROTATING CYCLIC-TORQUE SLIP TEST

The objective of this test was to determine the cyclic torque at which the clutch fails to reengage. This test was performed on the selected candidate clutch only, Design D.

A steady torque of 45,540 in.-lb and an alternating load of $\pm 4,560$ in.-lb were applied. The alternating torque was increased in increments of $\pm 3,000$ in.-lb and run for 5 minutes at each setting or until the clutch began to slip.

The following data was monitored and recorded at each load level:

- Static torque load in.-lb, ± 120 in.-lb
- Alternating torque load in.-lb, ± 600 in.-lb
- Angular displacement degrees, ± 5 degrees

STATIC CYCLIC-TORQUE FATIGUE TEST

The objective of this test was to determine the fatigue characteristics of the clutch. This test was performed on clutch Design D only.

A static torque of 91,000 in.-lb and an alternating torque of $\pm 13,600$ in.-lb were applied. The test was to run for 10 million cycles or until failure. The following data was recorded in 500,000-cycle increments:

- Torque loading in.-lb, ± 120 in.-lb
- Number of cycles $\pm 1,000$ cycles
- Angular displacement degrees, ± 5.0 degrees

50-HOUR DIFFERENTIAL-SPEED ENDURANCE TEST

The objective of this test was to determine the ability of the clutch to function properly under adverse flight conditions for a sustained period of time, to determine the wear characteristics and reliability, and to aid in the eventual establishment of a life cycle of the clutch. This test was performed on the selected candidate clutch only.

Data monitored was the same as that for the full-speed overrun test and was recorded at half-hour intervals.

Modifications to each clutch design and test reruns were made in accordance with Boeing Vertol test-plan document D301-10118-1 and were determined by the condition of the clutch and clutch races at the completion of the previous runs.

TEST DISCUSSION AND RESULTS

INITIAL CHECKOUT OF FIXTURE

The specimen clutch was housed between two tapered-roller bearings. During the initial assembly of the test-specimen cartridge, the bearings were installed with 0.005 to 0.001 inch of axial float. At the completion of a pretest run it was noted that there was light circumferential scoring on the tapered rollers and at the completion of the first 5-hour run, the bearing cage had failed as shown in Figures 20 and 21. Analysis of the failure indicated it was the result of the axial float and marginal lubrication. The assembly was modified to allow a greater oil flow through the bearings. The axial float was eliminated, and the bearings were preloaded from 1 to 5 in.-lb of running torque. In addition to these steps, the bearing cages were glass peened and silver plated to increase their marginal lubrication capability. No further difficulties were experienced with the tapered-roller bearings.

DETERMINATION OF OPTIMUM DESIGN

DESIGN A CLUTCH (BORG-WARNER X137661)

Full-Speed Test Run

Run 1 (6 gpm) of the full-speed overrun test was successfully completed with wear of 0.005 to 0.002 inch noted on the outside diameter of the outer drag strips in the area of contact with the clutch outer race. Inspection at the end of run 2 (4 gpm) revealed wear of 0.008 inch on the bend radii of the inner drag strips where they made contact with the clutch inner cage (Figure 22). There had been very little experience with wear in this area on clutches currently in service with similar configurations. As a result of the excessive wear, the inner drag strips were replaced with lower spring-rate strips. The clutch was then subjected to 30 minutes at 6 gpm and 5 hours at 4 gpm flow. Inspection after this run showed no signs of wear. The clutch then completed run 3 (2 gpm) and run 4 (1.3 gpm) of the full-speed overrun tests with no signs of distress. Drag-strip wear was within the acceptable limits of 0 to 0.0005 inch as determined by final inspection.

Differential Overspeed Test

This testing was conducted at 2 gpm which represents 100 percent of the original design oil flow to the clutch. Testing on Design A clutch was terminated upon completion of run 1 of the differential-speed overrun test when it was noted that the sprags were scuffed at the inner-race contact and the clutch inner race exhibited at 0.0016-inch wear step (Figure 23).

BEARING CAGE



TAPERED-ROLLER BEARING ASSEMBLY



Figure 20. Cracking of Tapered-Roller Bearing--
Initial Assembly.

CIRCUMFERENTIAL SCORING AND EDGE LOADING ON ROLLER



EVIDENCE OF ROLLER SKIDDING ON INNER RACE

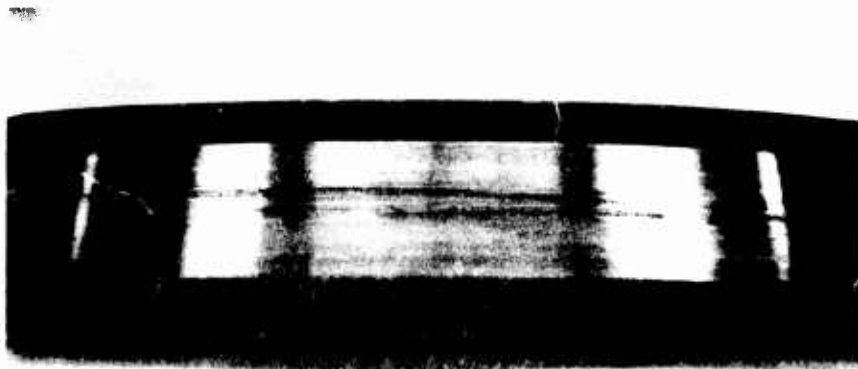


Figure 21. Surface Damage of Tapered-Roller Bearing.

INNER DRAG STRIP



OUTER DRAG STRIP

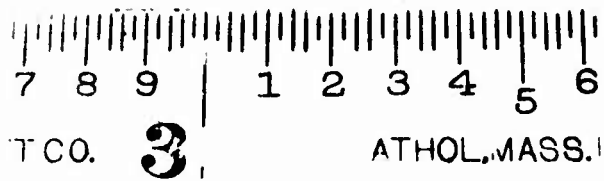


Figure 22. Wear on Outside Diameter of Design A Drag Strips.

INNER RACE--0.0016-IN. WEAR STEP



SPRAG--SCUFFED



OUTER RACE--NO DISCREPANCY

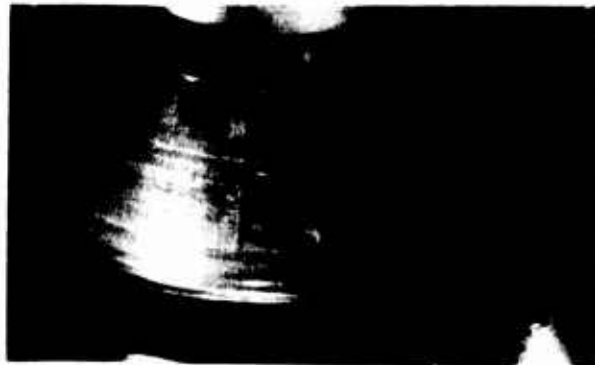


Figure 23. Design A Components After 50-Percent Differential-Speed Overrun Test.

A test summary is shown in Table III. Inspection of the inner-drag-strip showed that wear was considerably reduced. Sprag scuffing is believed to be the result of a very high rubbing force on the inner race as exhibited by the high heat-rejection rate and high drag torque shown in Figures 24 through 27.

DESIGN B (BORG-WARNER X137675)

Full and Differential Speed Tests

As originally received, Design B contained sprags having the same strut angle as Design A. Since the results of the previous test (Design A) indicated that the rubbing force was too high, sprags with a lower center-of-gravity offset were installed before starting tests on this design. This clutch successfully completed all full and differential overrun tests, as shown in Table III.

Additional Nonscheduled Testing

The completion of this testing, an additional test at 2 gpm was performed to determine if the clutch would become centrifugally disengaged at high speed due to the low center-of-gravity offset sprags. Disengagements and re-engagements were successfully accomplished at speeds from 7,600 to 9,500 rpm. Due to greater rubbing forces at higher speeds and the fact that there were no provisions for the application of an external force to initiate the disengagement, slippage could not be induced at speeds above 9,500 rpm. Inspection at the completion of this test revealed a 0.0005-inch wear step on the inner race under one row of sprags only, shown in Figure 28; there were no apparent discrepancies on the second row of sprags. A dimensional inspection of the clutch by the manufacturer indicated that there was no geometric or metallurgical discrepancy apparent on the sprags, and that the light scoring under one row of sprags could possibly be attributed to foreign debris and/or slightly marginal lubrication.

The marginal oil was attributed to the adjacent oil retainer (ST40869-2) with the ID being larger than the clutch shaft (ST40872-1) inner race OD (Figure 10). This oil retainer to shaft clearance was necessary to allow assembly and disassembly operations. Ideally, the clearance between the oil retainer and shaft should be small enough to keep sufficient oil in the clutch area. However, optimum clearances could not be obtained in that dam, since, reducing the clearances would have meant damaging the clutch inner-race on assembly. The alternative of this solution was to increase the amount of oil flow to the clutch from the original design value of 2 gpm to 4 gpm which was the final design value of oil flow to the clutch.

Of the three designs tested, Design B exhibited the best performance as is evidenced by the drag torque and heat rejection rates shown in Figures 24 through 27.

TABLE III. SUMMARY OF OPTIMIZATION TESTING

Test	Running Time (hr)					
	Design A		Design B	Design C		Design D
	Stock	Reconfigured ^a		Stock	Reconfigured ^c	
Full-Speed Overrun Test						
Run 1--6 GPM Oil Flow	5	0.5	5	5	-	5
Run 2--4 GPM Oil Flow	5	5	5	5	-	5
Run 3--2 GPM Oil Flow	-	5	5	5	-	5
Run 4--1.3 GPM Oil Flow	-	5	5	5	-	5
Differential-Speed Test at 2 GPM Oil Flow (Design A,B, and at 4 gpm (Design D) C)						
Run 1--50 Pct Design Speed	-	^b 1	1	1	0.25	1
Run 2--67 Pct Design Speed	-	-	1	1	0.25	1
Run 3--75 Pct Design Speed	-	-	1	^b 1	1	1
Endurance Run at 4 GPM Oil Flow and 75 Pct Design Speed	-	-	-	-	-	50
Additional Engagement Tests (2 gpm)						
^a Replaced inner drag strips with lower-load strips						
^b Failed						
^c Installed new clutches with lower center-of-gravity offset sprags						

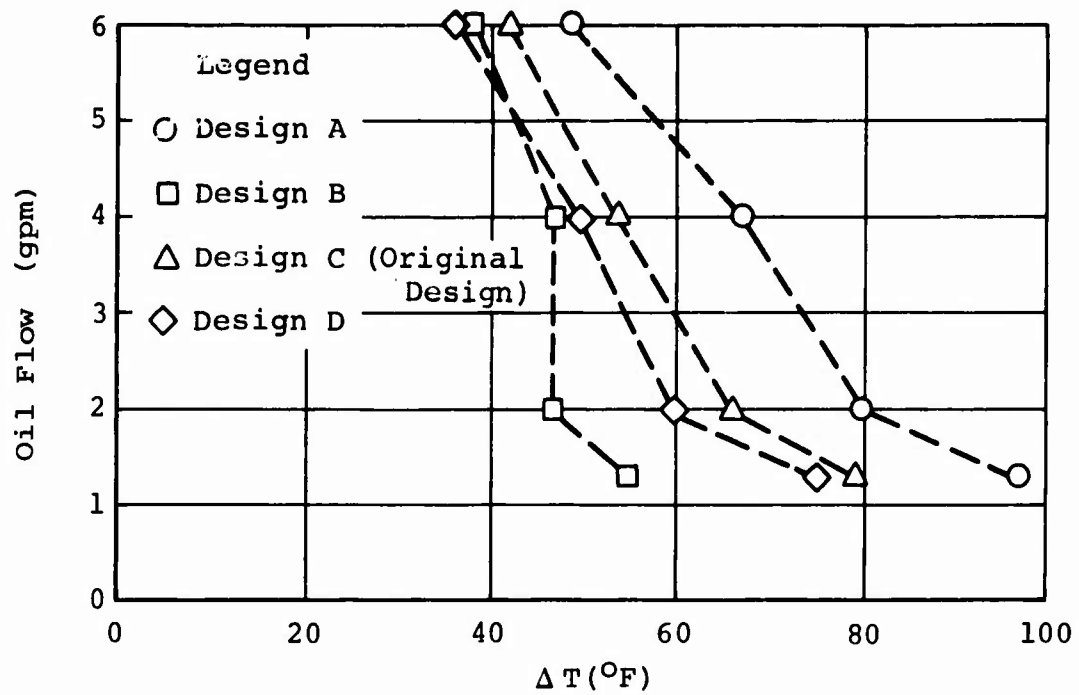


Figure 24. Heat Rejection Versus Oil Flow at 100-Percent Overrunning.

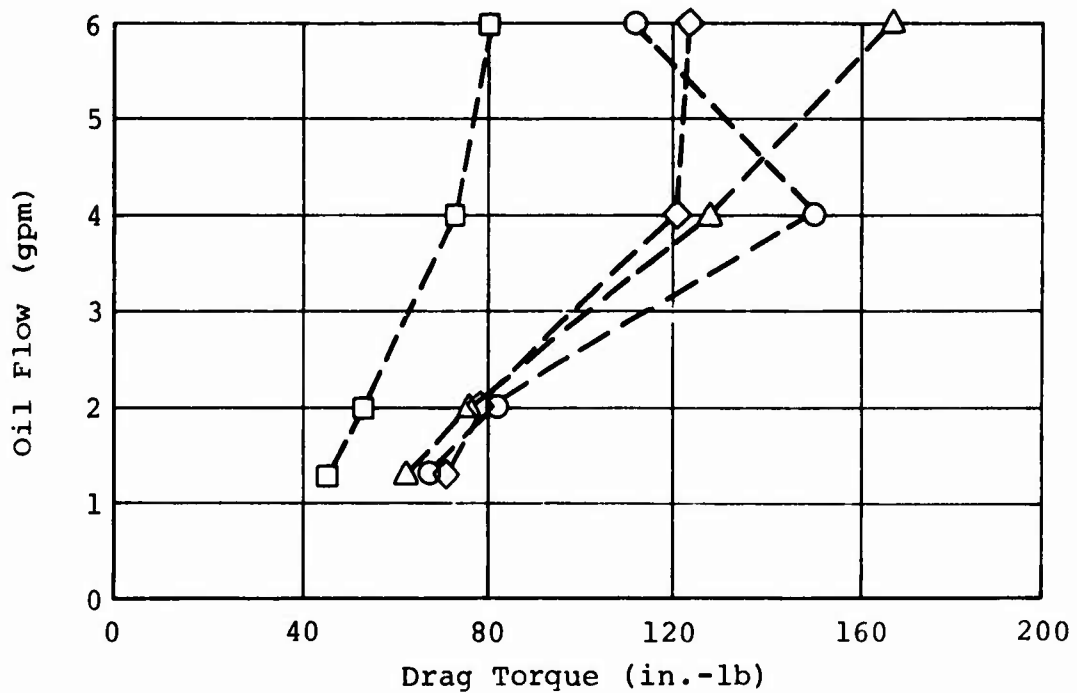


Figure 25. Drag Torque Versus Oil Flow at 100-Percent Overrunning.

Legend

- Design A 2 gpm
- Design B 2 gpm
- △ Design C 2 gpm (Original Design)
- ◇ Design D 4 gpm
- ◇ Design C 2 gpm (low CF Sprag)

F = Failure Test Terminated

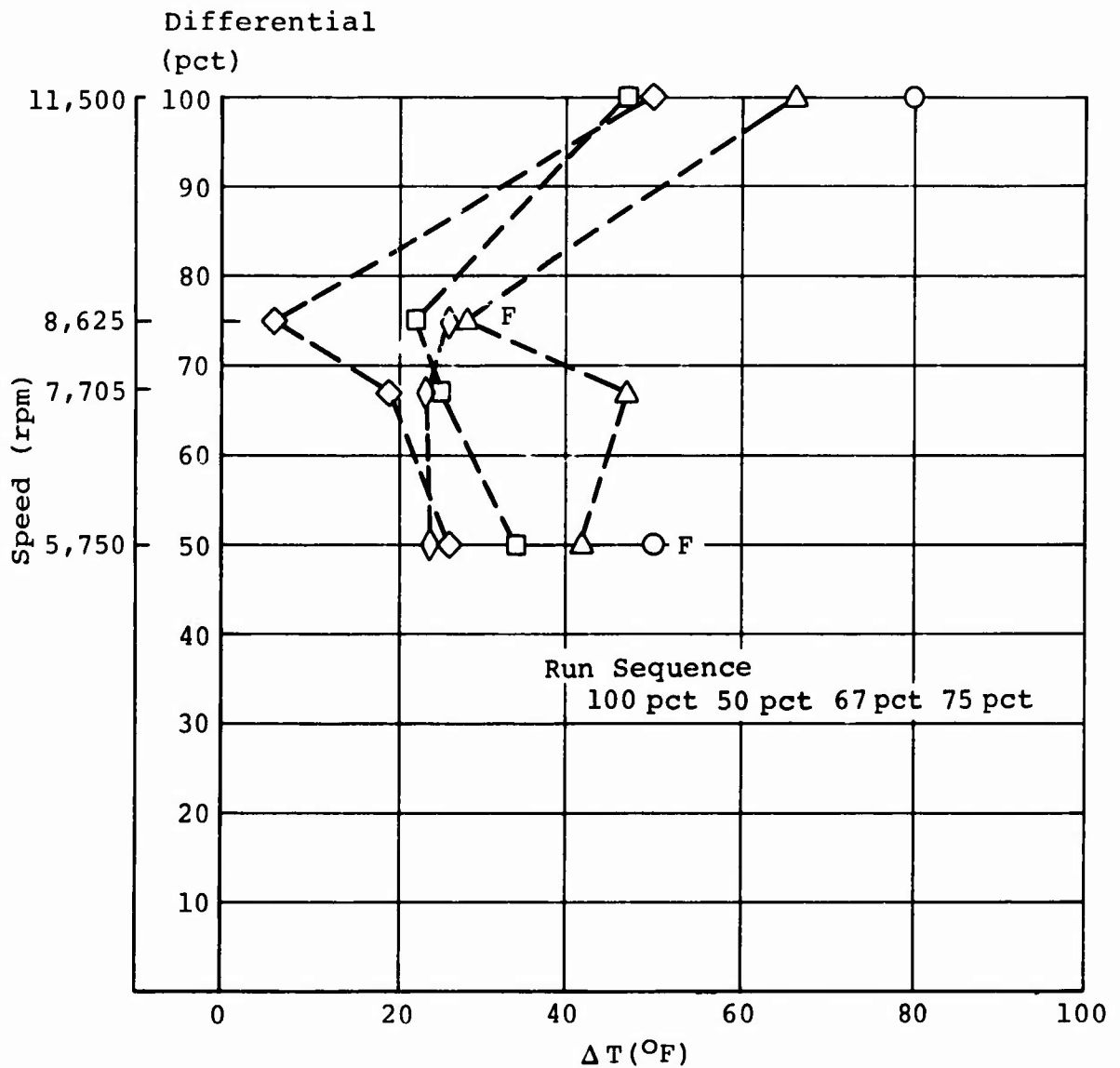


Figure 26. Heat Rejection Versus Differential Speed Overrunning.

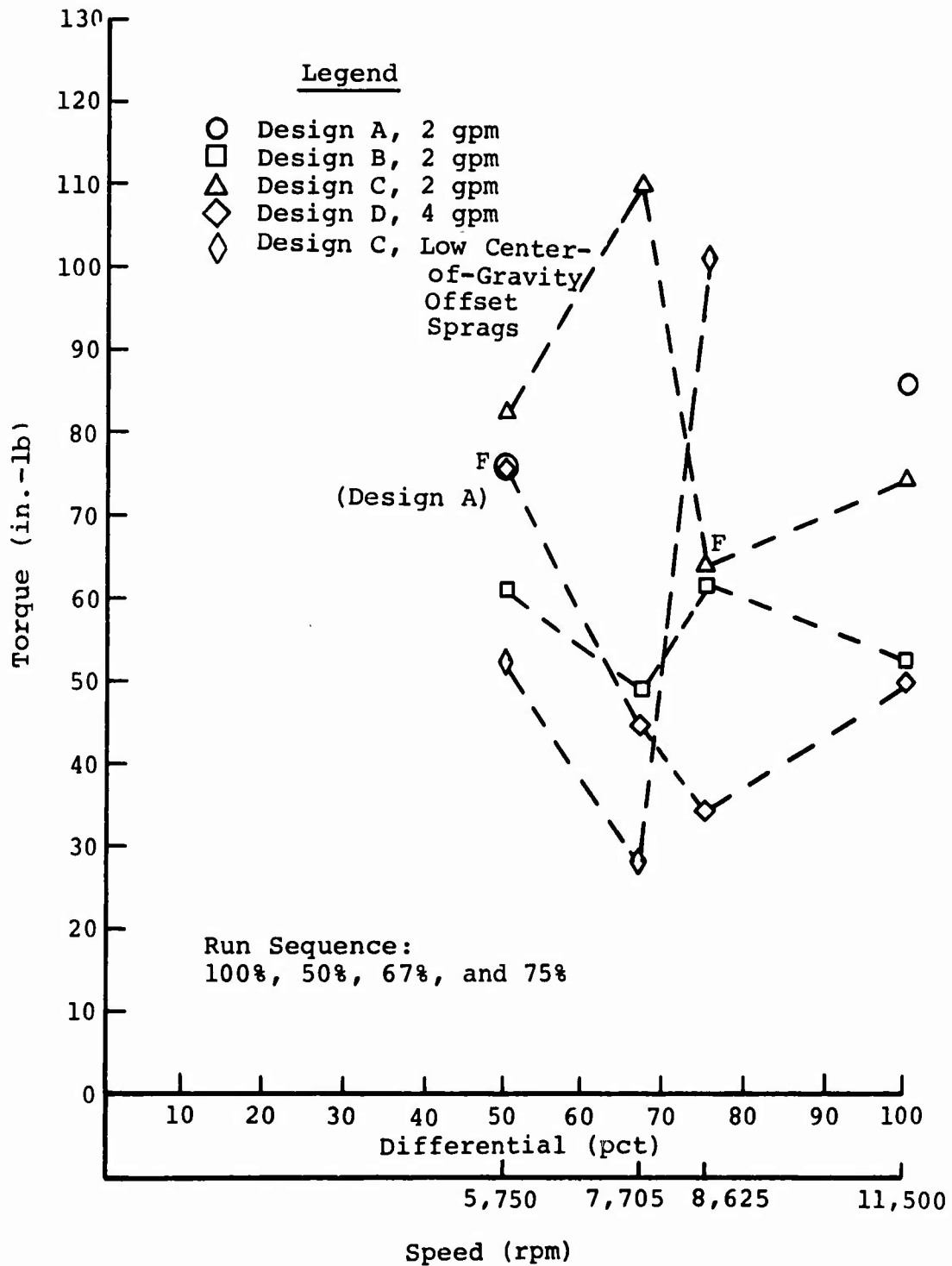


Figure 27. Drag Torque Versus Differential Speed.



Figure 28. Design B Clutch Shaft Exhibiting 0.0016-Inch Wear on Inner Race After Disengagement Test.

DESIGN C (FORMSPRAG CL-41802)

Full and Differential Speed Overrunning Tests

Design C successfully completed all of the full overrun and runs 1 and 2 of the differential-speed overrun tests, as indicated in Table III. At the completion of the third differential-speed overrun test, the clutch inner race was severely scored, with 0.0045 inch of wear step and the inside diameter of the sprags was scuffed (Figure 29). The distress on the clutch and inner race is indicative of high rubbing forces. Testing on this configuration was terminated and a new set of clutches incorporating standard garter springs and sprags with a lower center-of-gravity offset were installed. Run 3, the 75-percent differential-speed overrun test, was again performed. Inspection at the completion of this test revealed light polishing of the inner race; however, there was no measurable wear or sprag distress (Figure 30).

Additional Testing

A test to determine if the clutch would become centrifugally disengaged was performed at input shaft speeds from 6,800 to 11,500 rpm. The clutch did not disengage; however, during a routine test-stand shut down, it was noted that at approximately 860 rpm input speed, the clutch slipped and then re-engaged at about 470 rpm. Two additional shutdowns were effected with the same results; however, at the completion of the high-speed disengagement test, this phenomenon did not occur. Before removal at the completion of the high-speed



INNER RACE--0.0045-IN. WEAR STEP

SPRAG--SCUFFED



Figure 29. Design C Components After 75-Percent Differential-Speed Overrun Test.

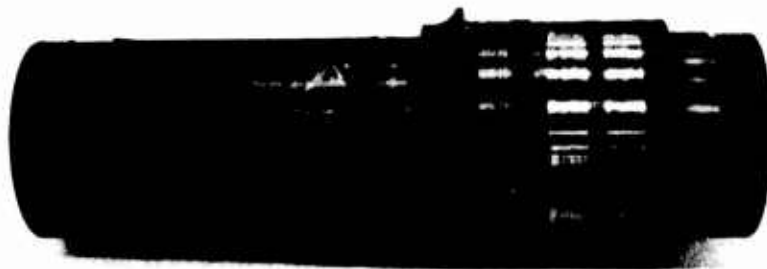


Figure 30. Design C Inner Race After Differential-Speed Test With Low Center-of-Gravity Offset Sprags.

disengagement test, data was recorded at 50, 67, and 75 percent differential speeds with the reconfigured clutch.

Design C exhibited a high heat-rejection rate during the full-speed overrun and the differential-speed overrun tests (Figures 24 through 27). Changing to the low center-of-gravity offset sprags reduced the heat-rejection rate at 50 to 67 percent differential speed, but at 75 percent the rate was slightly higher.

Figure 31 summarizes the evaluation testing conducted on clutch Designs A, B, and C, and Figure 32 shows the test clutches together with the inner-race shafts at completion of these tests.

TESTING OF OPTIMIZED DESIGN D

Full and Differential Speed Overrunning

The optimum Design D (Borg-Warner X137920), which is similar to Design B (Borg-Warner X137675), except for the addition of inner drag at strips as included in Design A (X137661), was configured after analysis of the data from the previously tested clutches and consideration of the HLH aircraft requirements. The best features of each clutch with modifications and additions as required were incorporated into Design D. The bend radii of the inner and outer drag strips were increased to improve the wear characteristics in this area. The flattened bend radii showed no measurable wear at the completion of the 50-hour endurance test, as shown in Figures 33 and 34. Design D successfully completed the entire series of the full- and differential-speed overrun tests of Table III. The differential-speed overrun tests were run with a 4-gpm oil flow in accordance with the conclusions reached during the disengagement testing of clutch B which showed lower oil flows to be marginal. This represents 100-percent of the final design oil flow to the clutch. No discrepancies were noted throughout the entire test series.

The heat-rejection rate and the magnitude of the drag torque of Design D in comparison with the other clutches tested are shown in Figures 24 through 27.

Endurance Testing

A 50-hour 75-percent differential-speed endurance test with a 3 gpm oil flow was conducted on this clutch. An oil flow rate of 3 gpm was chosen in lieu of the final design oil pump output of 4 gpm in order to evaluate and determine if there is a sufficient margin of lubrication. At the completion of the endurance test, inspection of the clutch revealed:

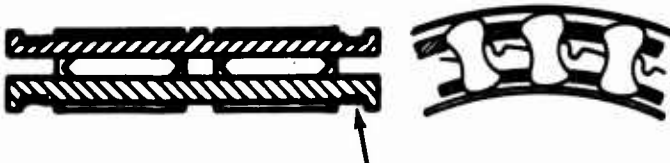


	Full Overrun	Differential Overrun
<p>Design A</p>  <p>Inner-Race Drag Strips</p>	<ul style="list-style-type: none"> • Complete Drag-Strip Wear Solved by Redesign 	<ul style="list-style-type: none"> • Failed Test at 50% Differential
<p>Design B</p>  <p>No Drag Strips Redesigned Sprags</p>	<ul style="list-style-type: none"> • Complete No Failures 	<ul style="list-style-type: none"> • With Redesigned Sprags, Passed 50% 67% and 75%
<p>Design C</p>  <p>Tested With and Without Redesigned Sprags</p>	<ul style="list-style-type: none"> • Complete No Failures 	<ul style="list-style-type: none"> Passed 50% and 67% Failed at 75% • With Redesigned Sprags Passed 75%

Figure 31. Summary of Clutch-Evaluation Testing.

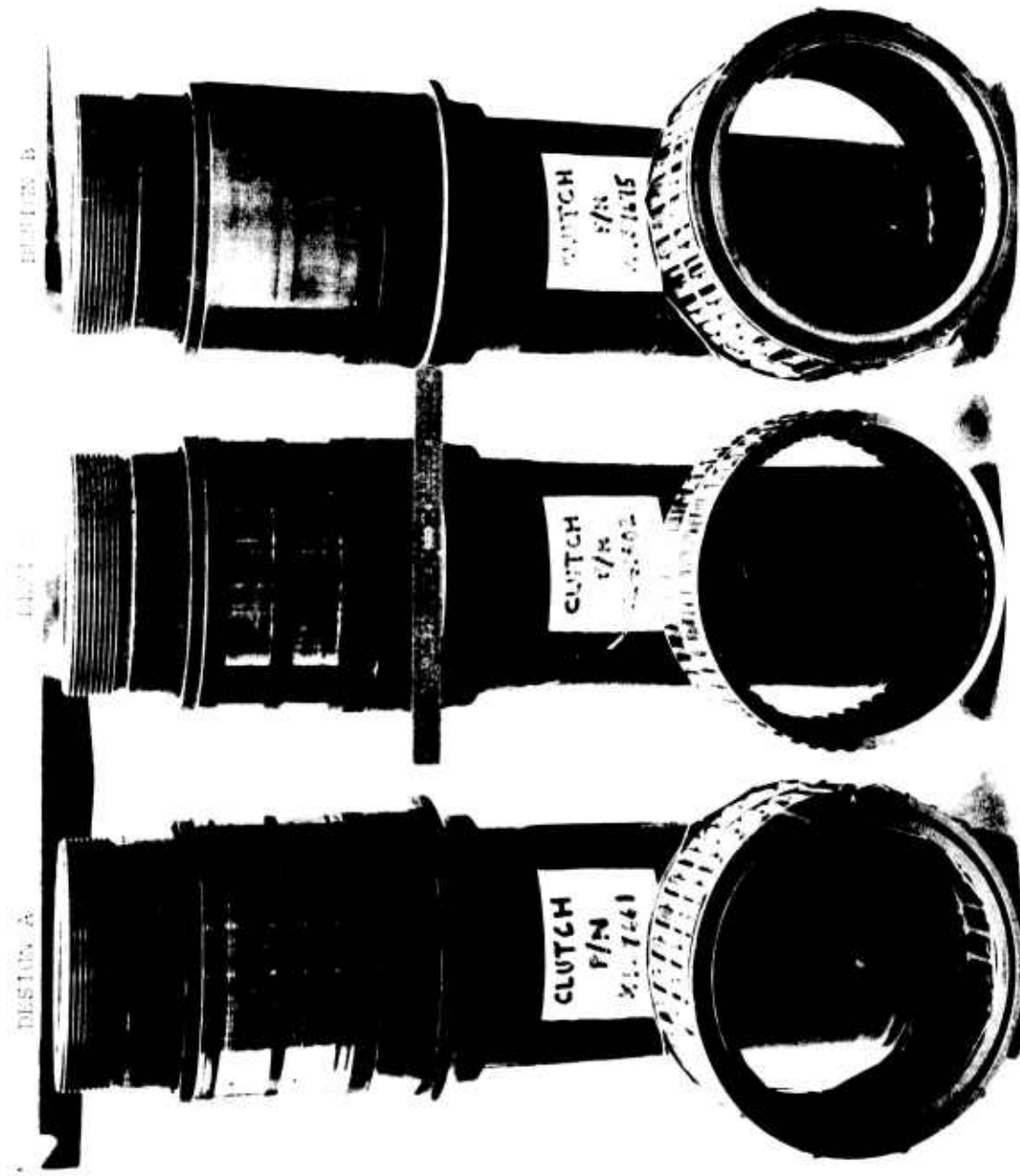


Figure 32. Clutches and Inner-Race Shafts After Evaluation Testing.



Figure 33. Design D Inner Drag Strip, Showing No Wear After 50-Hour Endurance Test.



Figure 34. Design D Outer Drag Strip Showing No Wear After 50-Hour Endurance Test.

- A 0.0002-inch wear path on the inside diameter of the sprags
- Several breaks in the energizing ribbons (Figures 35 and 36)
- No wear on the clutch inner race (Figure 37)

The indexing of the energizing ribbons and inner and outer cage pockets was checked and found to be within tolerance. The energizing ribbon radii were checked and found to be slightly irregular.

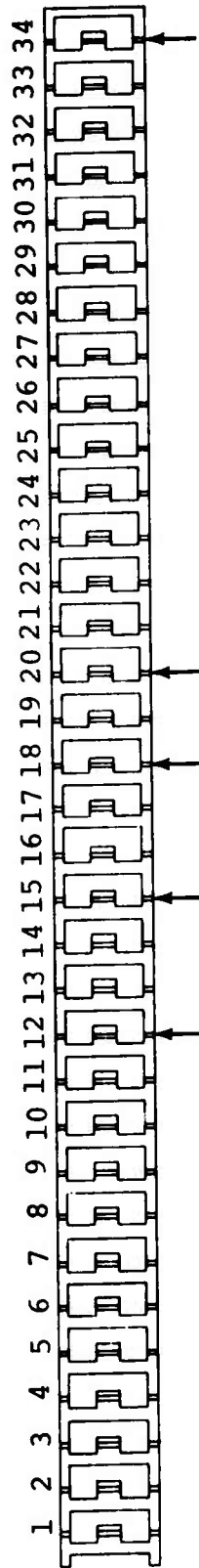
Static Testing

In addition to the dynamic testing performed on the candidate clutch, Design D, the following tests were performed. For the nonrotating cyclic-torque slip test, the clutch assembly and bearings were packed in MIL-G-81322 grease. During the initial loading and instrumentation systems checkout with a static load of 45,540 in.-lb and an alternating load of $\pm 4,560$ in.-lb applied, slippage occurred immediately. The loads were increased to 91,000 in.-lb $\pm 9,000$ in.-lb, and slippage continued to be excessive. The clutch assembly was removed, disassembled, and degreased; inspection revealed no discrepancies. The test cartridge was reassembled using the same parts but using MIL-L-7808 oil as a lubricant. The slippage rate had improved but not to the point of satisfaction, and a second disassembly and inspection was performed; no significant wear was apparent. A new clutch and inner race were assembled and reinstalled in the test stand. The new assembly was lubricated with MIL-L-7808 oil. Retesting showed that the slip rate had decreased over the previous clutch assemblies (Figure 38).

A frequency sweep from 10 Hz to 30 Hz with 91,000 in.-lb steady and $\pm 9,000$ in.-lb alternating torque applied was performed to determine if a resonant condition existed, thereby causing the slippage. No angular displacement between the inner and outer races was indicated. There was no amplitude or phase shifts throughout the entire sweep indicating that no detrimental resonance was present within the limits checked.

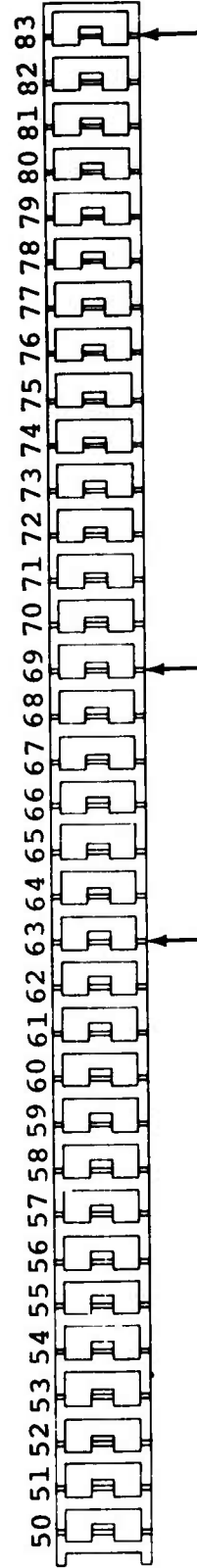
Because Design D was not available for test at this time and the geometric configuration of the cages, sprags, energizing ribbons, and drag strips of clutch Design A were similar to those ordered for Design D, all of the above static testing was performed on Design A.

At this point it was decided to hold the nonrotating cyclic-torque slip test in abeyance until Design D was received and to proceed to the nonrotating cyclic-torque fatigue test. This test was performed with a steady load of 91,000 in.-lb and an alternating torque of $\pm 13,600$ in.-lb applied to Design A. It was noted that the slip rate decreased as the cyclic count increased beyond 250,000. At 500,000 cycles, slippage stopped



Arrows Indicate Points of Failure

Figure 35. Map of Failures of Design A Energizing Ribbon After 50-Hour Endurance Testing.



Arrows Indicate Points of Failure

Figure 36. Map of Failures of Design D Energizing Ribbon After 50-Hour Endurance Testing.



Figure 37. Design D Inner Race, Showing No Wear After 50-Hour Endurance Test.

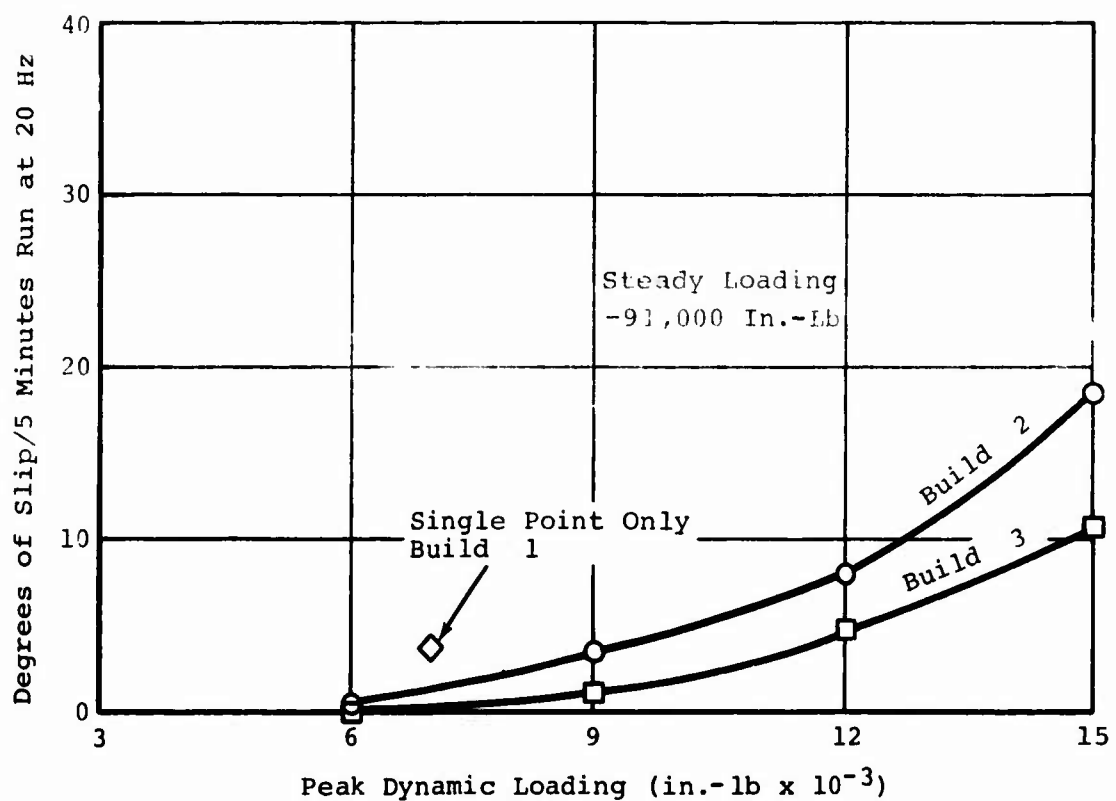


Figure 38. Results of Slip Test.

(Figure 39). The clutch completed 10 million cycles with no further slippage and no indication of distress.

Without the benefit of a post-fatigue-test teardown and inspection, the nonrotating slippage test was performed. A steady load of 45,500 in.-lb and an alternating load of $\pm 3,000$ in.-lb was applied. The alternating load was increased in increments of 3,000 in.-lb. The clutch assembly was then subjected to a 5-minute test at each incremental load level. At the $\pm 18,000$ in.-lb alternating load level, the clutch began to slip at the rate of 6 deg/min. Inspection at the completion of testing revealed several fatigue-induced cracks emanating from the sharp pocket radii of both the inner and outer clutch cages. There was light fretting on the sprag contact area and pronounced fretting on approximately 180 degrees of the silver-plated pilot surface of the inner cage (Figures 40 through 44).

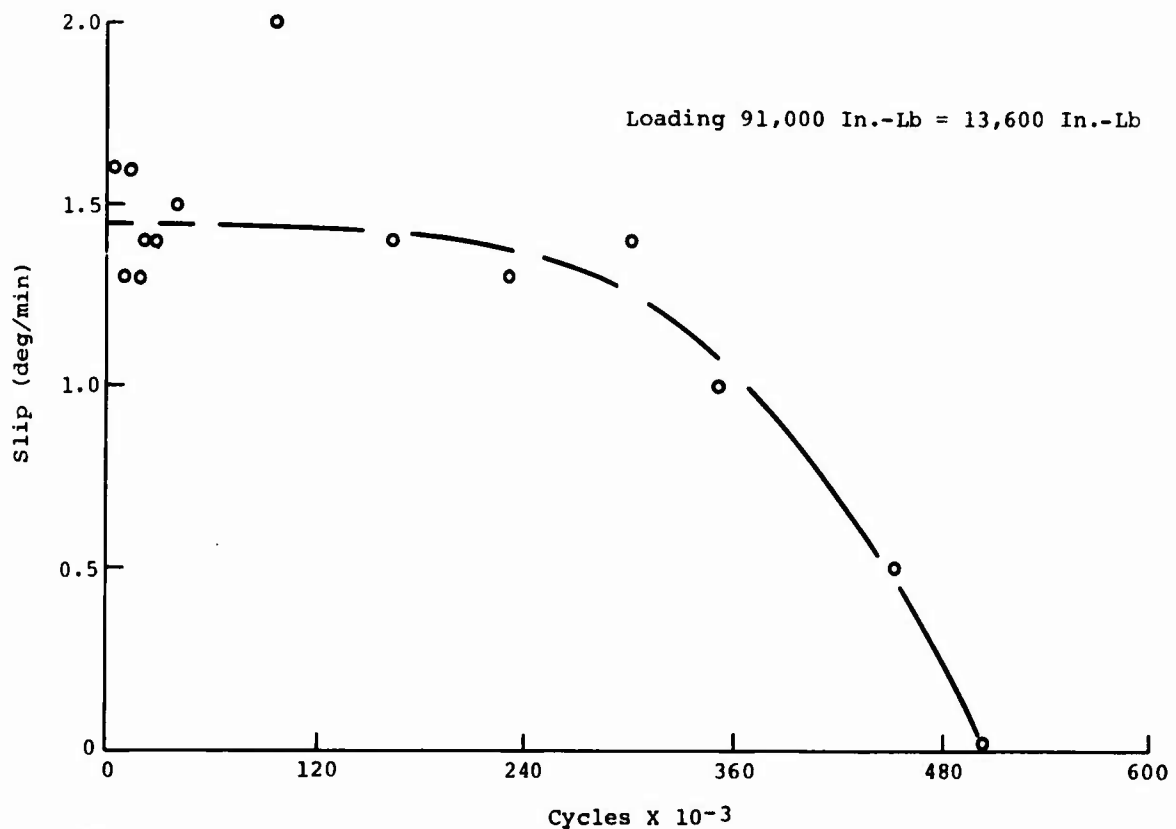
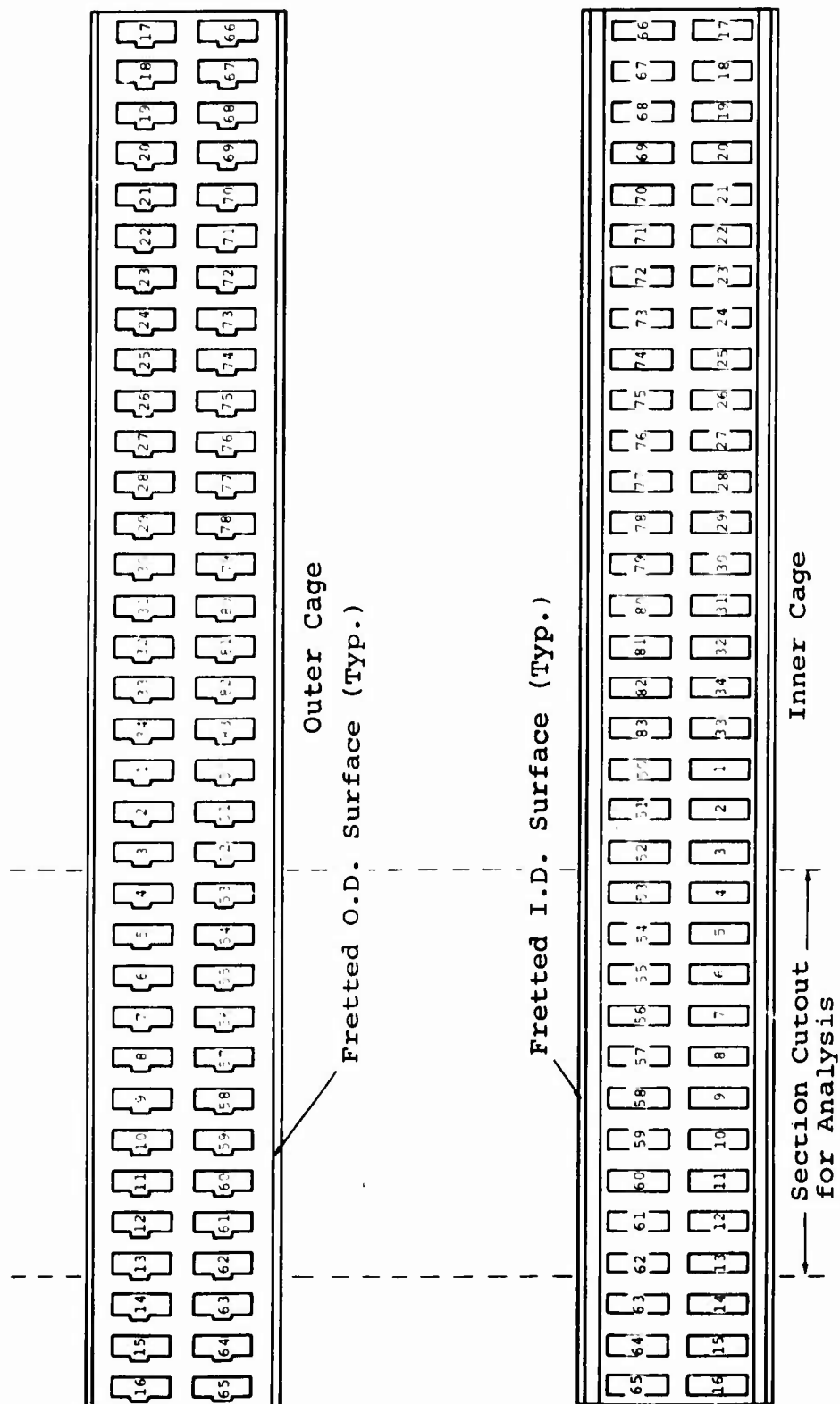
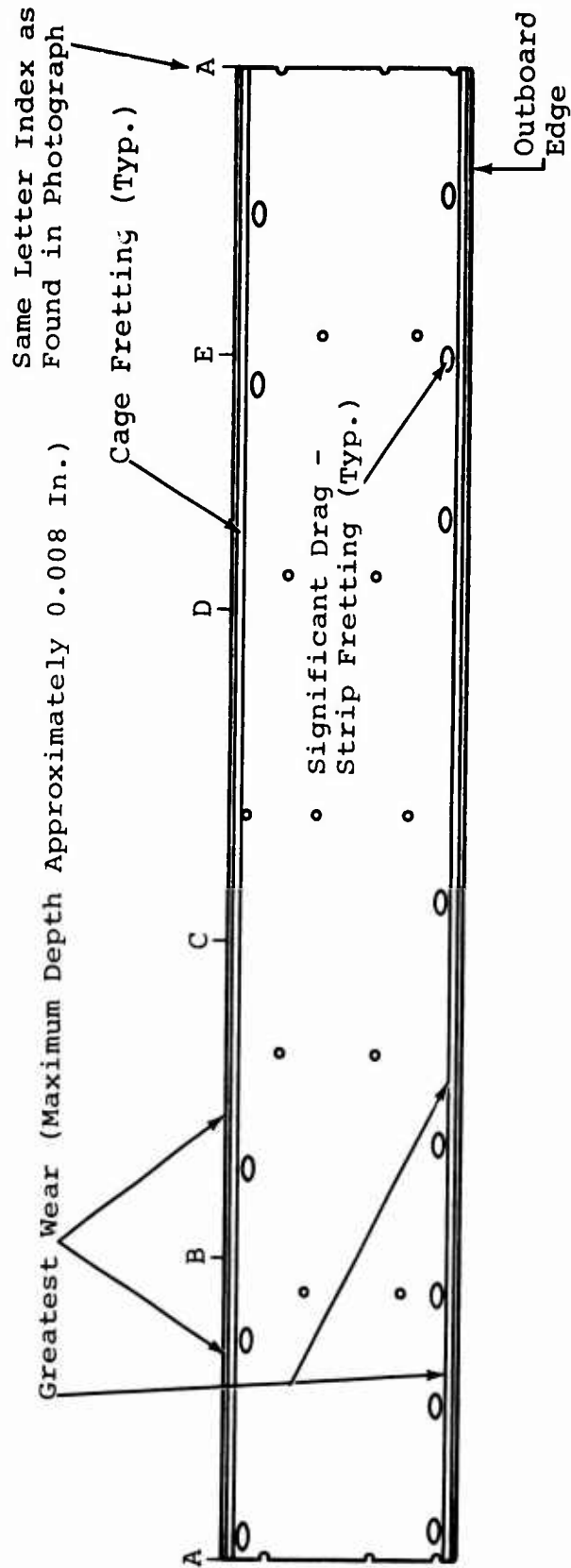


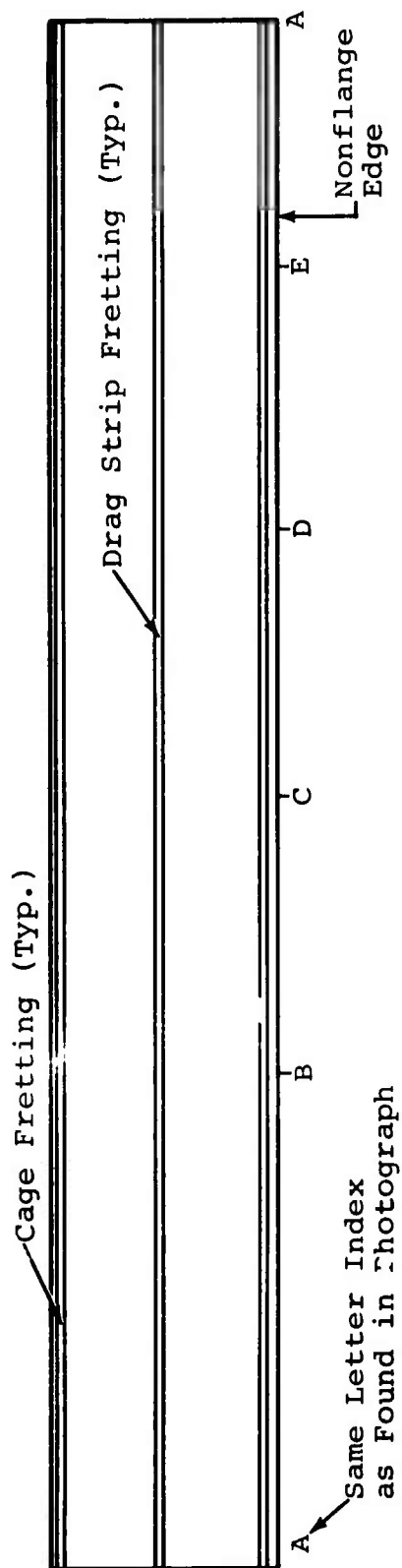
Figure 39. Results of the Nonrotating Cyclic-Torque Fatigue Test.





Note: Sprag contact is generally good. Poorest Surface is in the area of severe fretting by cage. Best surface is where there was no cage fretting.

Figure 41. Clutch-Shaft Fatigue Damage.



Note: Fretting on sprag contact and outboard drag strip surfaces was light.

Figure 42. Clutch-Housing Fatigue Damage.



Figure 43. Cracks on Outer Cage After Nonrotating Cyclic-Torque Fatigue Test--Assembly Similar to Design D.

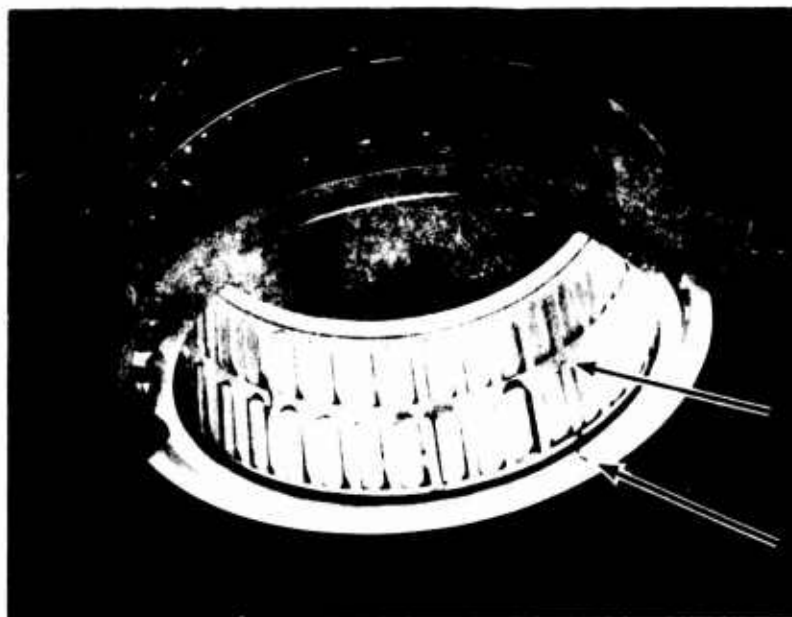


Figure 44. Cracks on Inner Cage After Nonrotating Cyclic-Torque Fatigue Test--Assembly Similar to Design D.

STATIC OVERLOAD TEST

This test was conducted on optimum clutch Design D only. The purpose of the test was to determine the clutch ultimate capacity. Static torque in the following increments was applied to the clutch by means of the test used in the previously described fatigue tests (Figure 18):

- 250 ft-lb from 0 to 4,000 ft-lb
- 500 ft-lb from 4,000 to 8,000 ft-lb
- 2,000 ft-lb from 8,000 ft-lb to failure

Failure was defined as roll over, slippage, or component fracture. Testing on one assembly only was conducted. All clutch parts including bearings were coated with grease (MIL-G-81322).

The following data was recorded at each torque setting:

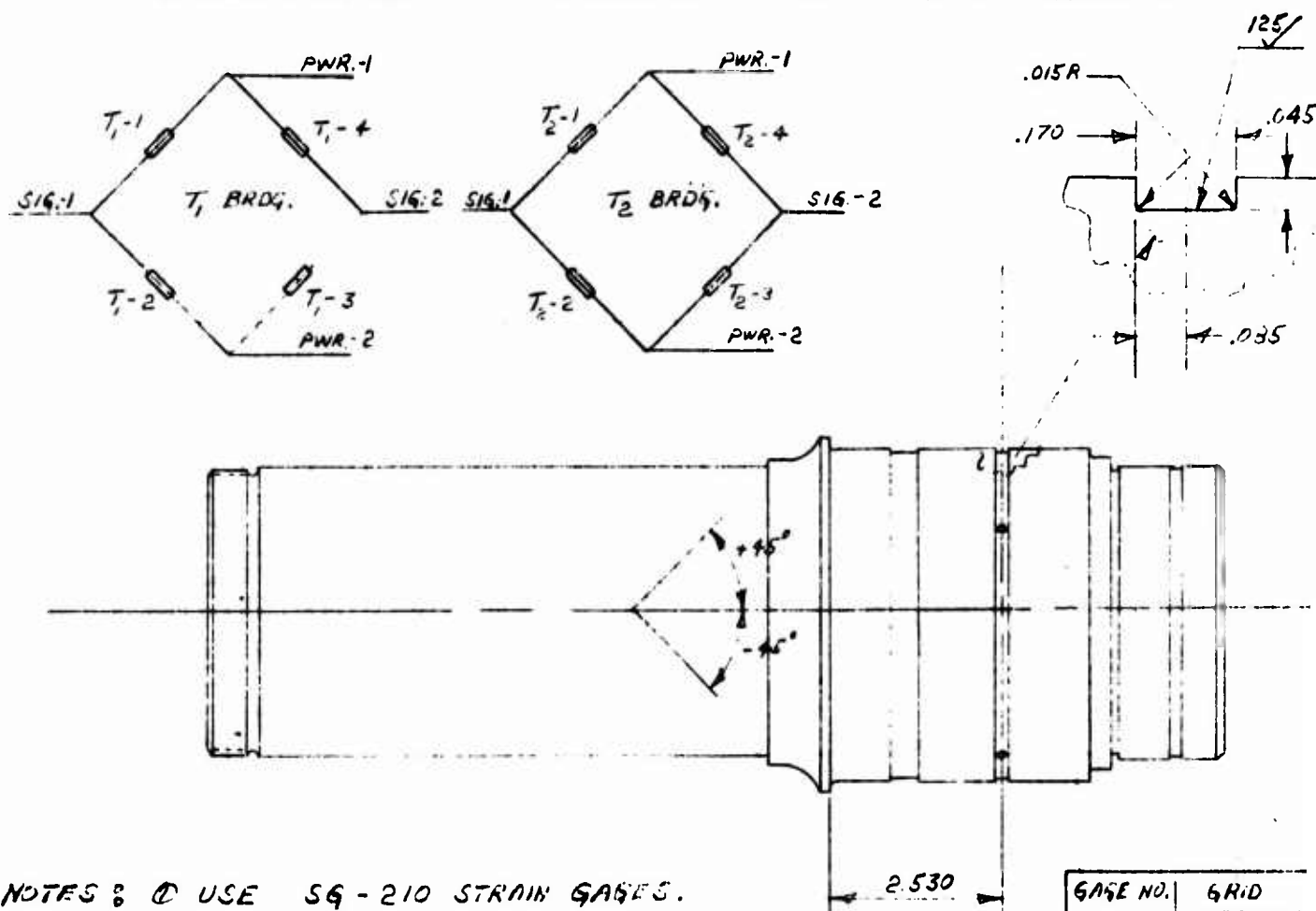
Torque ft-lb, ± 10 ft-lb
Angular displacement degrees, ± 0.5 degree
Outer-shaft deflection
 over each row of sprags -
 8 places total inches, ± 0.0005 inch
Load sharing between
 rows of sprags percent, ± 20 percent

All parts tested were used in previous overrunning and fatigue tests. All buildups for the static overload testing had less than 0.001-inch end-floating clearance. Subsequent teardowns revealed no change in this end clearance.

The load-sharing strain-gauged shaft (torsion bridge), Figure 45, was calibrated in two steps. In step 1, only clutch row 1 was installed in the buildup. See Figure 46 for row 1 location. Torque calibration, presented in Table IV, was done to 50 percent normal flight loading. In step 2, clutch row 1 was removed and clutch row 2 was installed in the buildup. Interaction data of row-2 compressive line contact strains interacting with the torsion gauges was also collected to 50 percent normal flight load, as shown in Table V.

The load-sharing test was done at 50 percent normal flight load. See Table VI for this data. Figures 47 and 48 are plots of the load-sharing data.

At various torque increments, while increasing torque to reach ultimate clutch failure, housing radial-deflection measurements were made across each row of sprags at four diameter locations spaced 45 degree apart. See Table VII for this data. Failure occurred at a torque level of 206,900 in.-lb or 17,240 ft-lb, which is equivalent to 468 percent of one-engine design torque.



NOTES: ① USE SQ-210 STRAIN GAGES.

② USE M-BOND 600 ADHESIVE. COAT WITH M-COAT A.

③ USE #28 AWG SPECTRASTRIP WIRE AND LABEL EACH LEAD TO ABOVE WIRING DIAGRAMS.

④ ROUTE ALL LEADS OUT $\frac{3}{8}$ " DIA HOLE IN CENTER OF SHAFT. LOCATE TERMINAL STRIPS AND ROUTE SOLDER-FLUX WIRE AS NEEDED TO MAKEUP T_1 & T_2 BRIDGES.

NOTE: THICKNESS OF GAGING MUST BE LESS THAN .045 SO AS NOT TO PROJECT ABOVE SHAFT SURFACE.

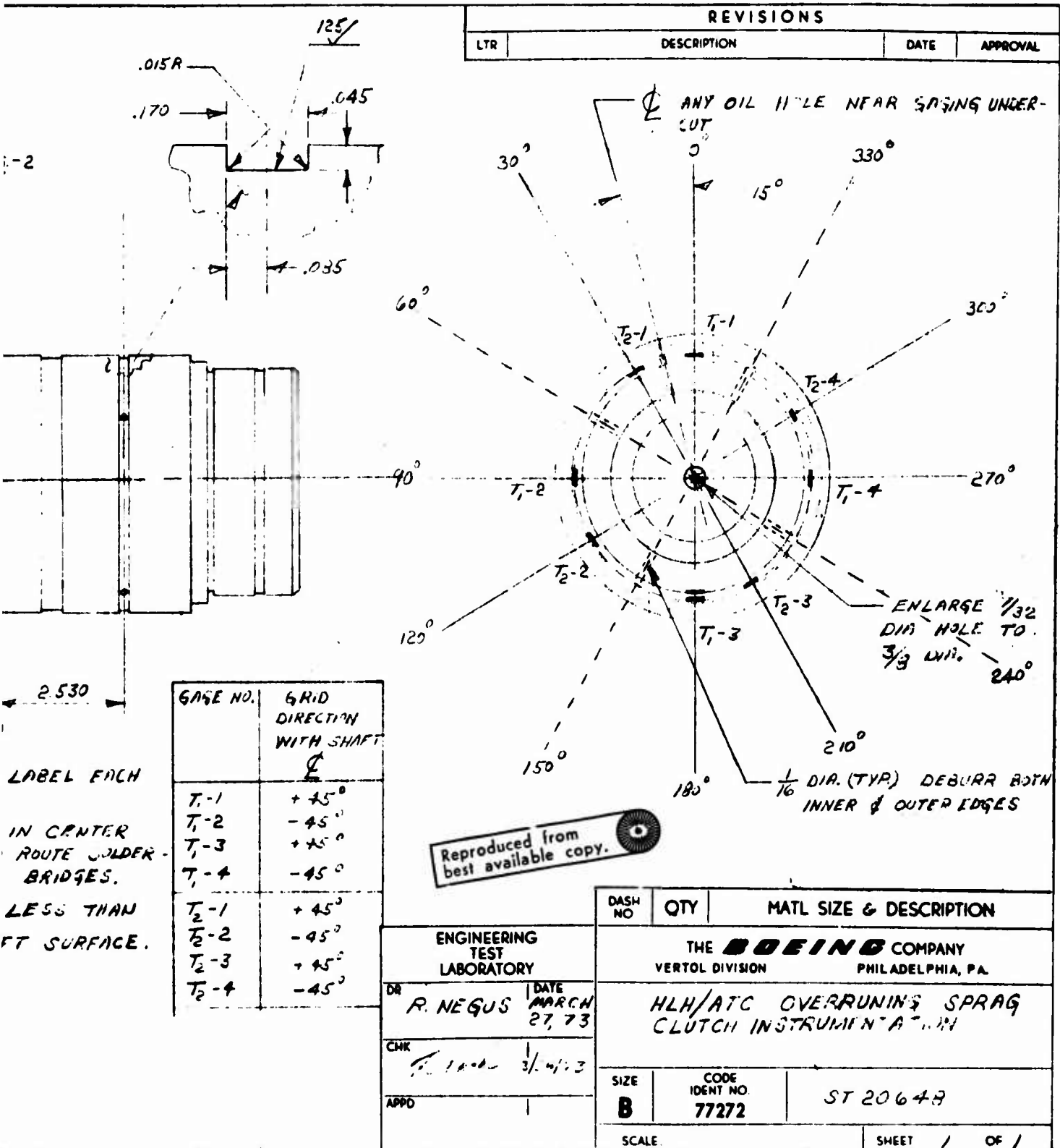
Reproduced from
best available copy.

GAGE NO.	GRID DIRECTION WITH SHAFT AXIS
T_1-1	+45°
T_1-2	-45°
T_1-3	+45°
T_1-4	-45°
T_2-1	+45°
T_2-2	-45°
T_2-3	+45°
T_2-4	-45°

* TERMINAL LOCATION ON END OF SHAFT IS OKAY.

Figure 45. Instrumentation for Sprag-Clutch Load-Sharing Static Test.

Preceding page blank



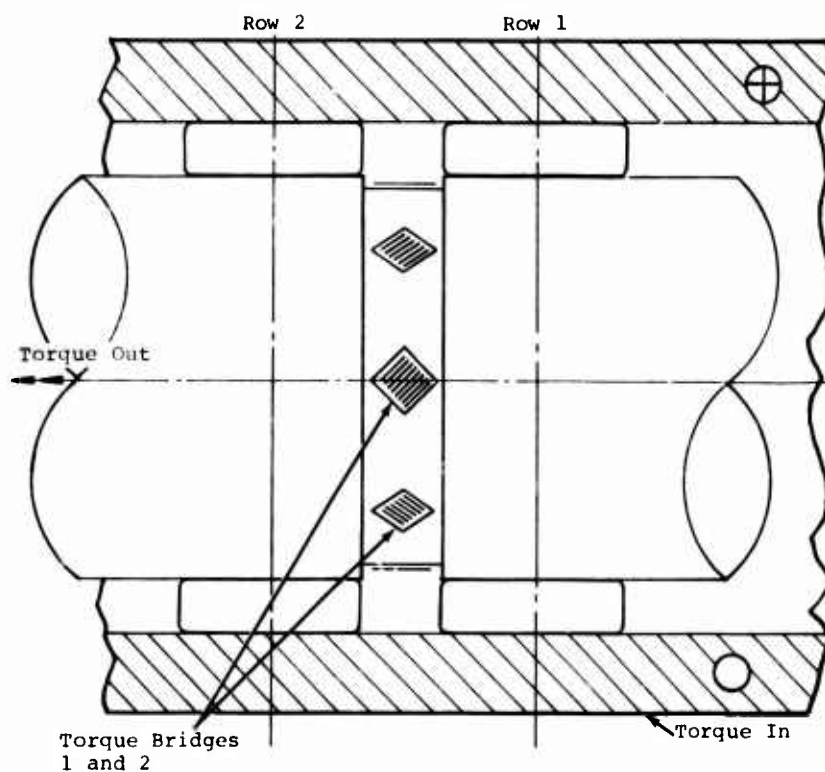


Figure 46. Load-Sharing Measurement Scheme.

TABLE IV. LOAD-SHARING CALIBRATION--ROW 1 ONLY			
Position*	Torque (in.-lb x 10 ⁻³)	Bridge Strain ($\frac{\text{in.}}{\text{in.}}$)	
		Bridge T-1	Bridge T-2
1	5.55	102	92
	11.10	200	182
	16.65	298	279
	22.20	396	368
	27.75	504	472
2	5.55	98	89
	11.10	204	182
	16.65	304	278
	22.20	401	376
	27.75	494	482
3	5.55	103	79
	11.10	208	165
	16.65	413	257
	22.20	421	348
	27.75	533	445
4	5.55	09	104
	11.10	207	207
	16.65	307	317
	22.20	397	410
	27.75	494	520
*Any random position			

TABLE V. LOAD-SHARING CALIBRATION--ROW 2 ONLY			
Position*	Torque (in.-lb x 10 ⁻³)	Bridge Strain ($\frac{\mu\text{in.}}{\text{in.}}$)	
		Bridge T-1	Bridge T-2
1	5.55	-14	-22
	11.10	-27	-43
	16.65	-57	-70
	22.20	-71	-81
	27.75	-87	-90
2	5.55	-16	-22
	11.10	-37	-46
	16.65	-56	-64
	22.20	-74	-81
	27.75	-92	-98
3	5.55	-25	-16
	11.10	-53	-35
	16.65	-80	-56
	22.20	-105	-77
	27.75	-131	-98
4	5.55	-22	-38
	11.10	-36	-68
	16.65	-47	-93
	22.20	-56	-120
	27.75	-65	-143
*Any random position			

TABLE VI. RESULTS OF LOAD-SHARING TEST			
Position*	Torque (in.-lb x 10 ⁻³)	Bridge Strain ($\frac{\mu\text{in.}}{\text{in.}}$)	
		Bridge T-1	Bridge T-2
1	5.55	78	50
	11.10	116	88
	16.65	154	134
	22.20	187	174
	27.75	224	215
2	5.55	46	35
	11.10	86	69
	16.65	125	107
	22.20	160	142
	27.75	195	180
3	5.55	49	32
	11.10	94	63
	16.65	141	94
	22.20	182	122
	27.75	222	153
4	5.55	33	37
	10.10	67	70
	16.65	100	99
	22.20	132	123
	27.75	169	148
*Any random position			

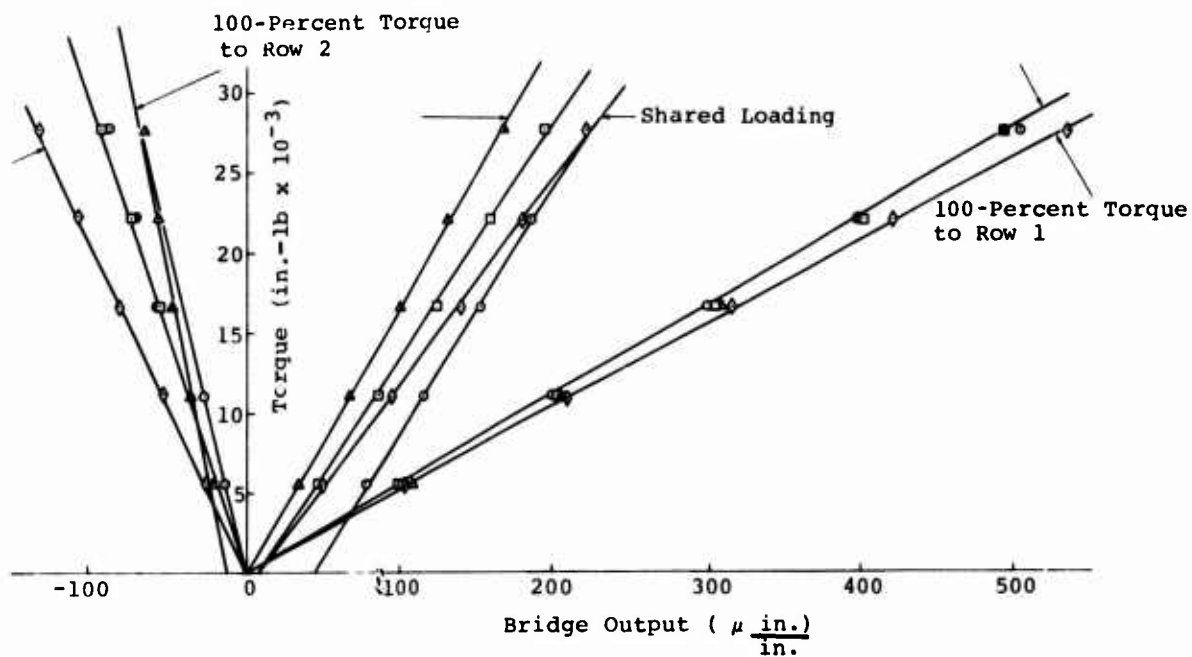


Figure 47. Results of Load-Sharing Clutch Test--T-1 Torque Bridge.

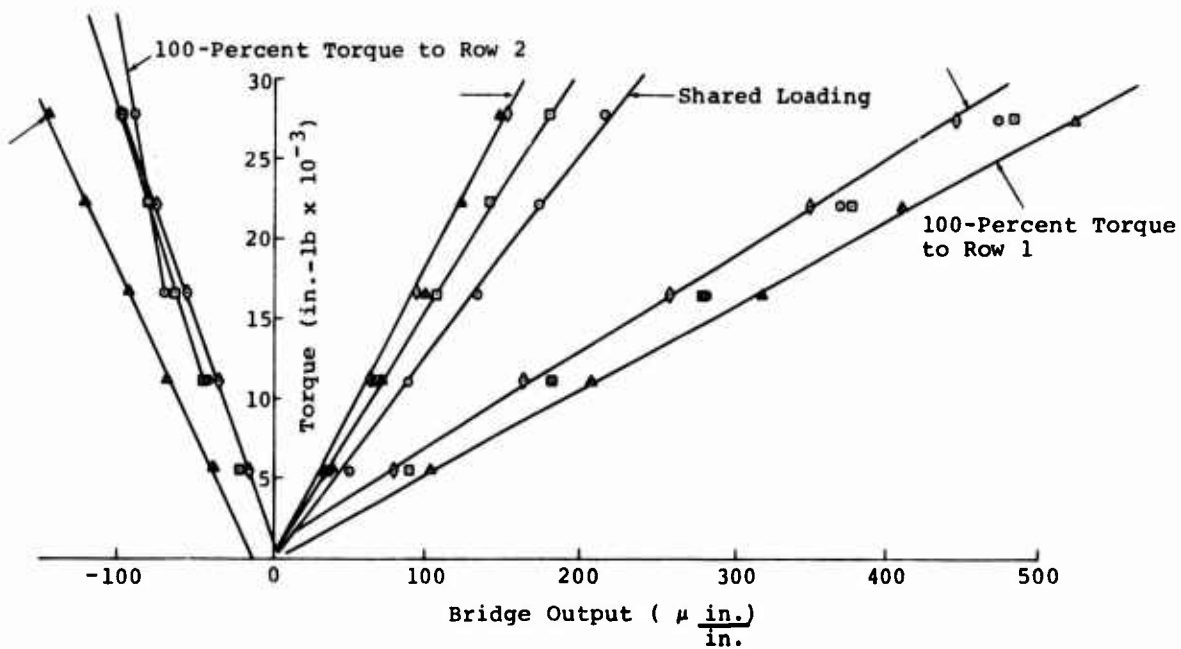


Figure 48. Results of Load-Sharing Clutch Test--T-2 Torque Bridge.

TABLE VII. HOUSING RADIAL DEFLECTION								
Torque (in.-lb x 10 ⁻³)	Housing-Diameter Increase (7.0xxx in.)							
	Row 1 Positions				Row 2 Positions			
	1	2	3	4	5	6	7	8
0	224	226	228	226	232	236	240	232
3	228	228	228	230	247	239	239	241
6	238	238	231	232	241	239	238	243
9	237	230	232	231	241	242	243	242
12	238	233	236	238	253	242	246	246
15	238	237	237	242	250	248	249	248
18	241	240	245	242	257	251	254	255
21	244	234	240	243	253	253	252	256
24	248	230	247	243	260	257	259	261
27	252	250	250	258	260	259	260	261
30	251	250	257	260	263	262	265	266
33	255	260	256	262	266	268	272	270
36	256	252	260	260	270	268	270	270
39	257	260	264	263	270	270	270	271
42	263	255	265	262	277	270	272	270
45	262	268	267	262	275	273	273	277
48	268	271	270	270	281	275	278	282
54	272	270	270	277	285	282	281	283
60	276	273	277	278	290	287	285	292
66	282	279	282	281	293	292	292	295
72	289	291	281	291	300	295	296	298
78	291	290	287	292	304	302	304	303
84	294	292	292	299	307	306	302	307
90	295	297	298	302	318	306	308	311
*90	302	300	303	303	319	311	312	318
96	301	302	306	302	321	318	318	321
120	320	320	328	322	331	331	330	332
144	332	343	337	344	352	345	352	350
207	Clutch failure (206,900 in.-lb)							
*New loading at a different position at start of another work day.								

The failure was sprag rolover. All sprag preload spring tabs but one were broken off. Also, several sprags had sheared "coffin corner" edges. Shaft and housing showed some brinelling. Unaided visual examination of the inner and outer cages revealed no damage (Figure 49).

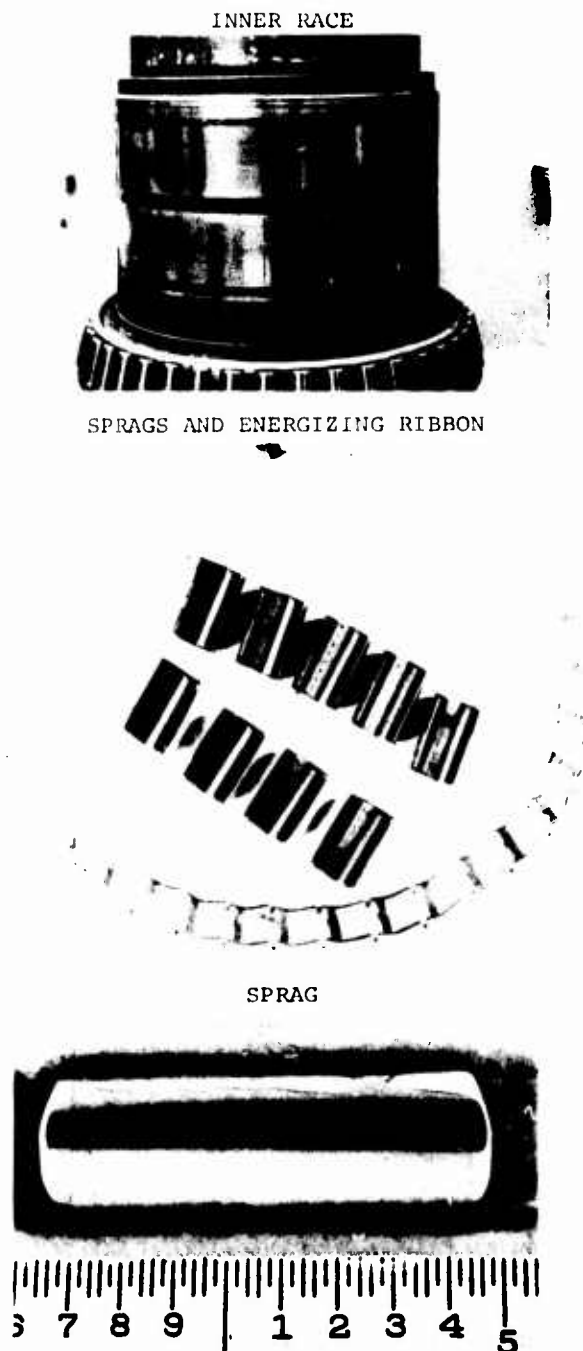


Figure 49. Design D Components After Static Overload Test.

Table VIII shows the results of the load-sharing test and indicates that on the average, each row carries approximately 50 percent of the torque.

TABLE VIII. SUMMARY OF LOAD-SHARING TEST RESULTS		
Position ^a	Torque Through Row 1 ^b (pct)	
	Torque Bridge 1	Torque Bridge 2
1	61.4	56.3
2	49.8	47.9
3	53.7	44.3
4	43.2	46.5
Average	52.0	48.8
^a Any random position ^b In the assembled position, row 1 is the first sprag-clutch row, looking from the engine end.		

CLUTCH ANALYSIS

The optimum test clutch, Design D (Borg-Warner X137920), and the HLH aircraft clutch (301-10629) have been analyzed by the methods presented in the appendix. Geometrical data required for the analysis was taken from the appropriate clutch raceway and sprag drawings and is presented in Table IX. Although the data was taken from the X137920-S aircraft sprag drawing, the X133366 test-clutch sprag is identical with respect to those dimensions used in the analysis. For analysis purposes, nominal values of all dimensions have been used. Note that the test and aircraft clutch configurations are identical with the exception of the outer-race thickness.

The results are presented in Figures 50 through 53. The curves extend to 100 percent cam rise, which indicates failure by sprag rollover. Table X presents the results as compared to the design criteria. The expected rollover torque for the aircraft clutch based on the test is also shown. Although this is slightly less than 450 percent torque, a problem with the aircraft clutch is not expected since the drive system ultimate torque is equivalent to 225 percent. Also, the outer-race hoop stress in the aircraft clutch is 3.5 percent above the criteria at 200 percent torque. However, since the test clutch completed 10 million cycles during the fatigue test at a torque level equivalent to 206 percent, ± 30.8 percent of aircraft single-engine torque without indication of outer race distress, and since the aircraft clutch operating condition is equivalent to 100 percent, ± 12 percent, of single-engine torque, the slightly higher calculated hoop stress does not indicate an objectionable condition. Note also that at clutch rollover, the outer-race hoop stress is less than the race ultimate tensile strength.

TABLE IX. CLUTCH GEOMETRY

Item	Design D	HLH Clutch
Inner-Race Part Number	ST40872	301-10629
Outer-Race Part Number	ST40870	301-10650
Sprag Part Number	X133366	X137920-S
Inner-Race Radius (R_i), in.	2.2545	2.2545
Outer-Race Radius (R_o), in.	2.7535	2.7535
Sprag Inner-Cam Radius (r_i), in.	0.265	0.265
Sprag Outer-Cam Radius (r_o), in.	0.278	0.278
Number of Sprags	34	34
Sprag Length (L), in.*	1.654	1.654
Effective Sprag Length (L_e), in.*	1.74	1.74
Inner-Race Thickness (t_i), in.	0.695	0.695
Outer-Race Thickness (t_o), in.	0.758	0.687
Sprag Thickness (t_s), in.	0.212	0.212
Available Cam Rise, in.	0.0235	0.0235
Eccentricity (e), in.	0.0485	0.0485
Eccentricity Angle (θ), deg	50.60	50.60
*Total of both rows		

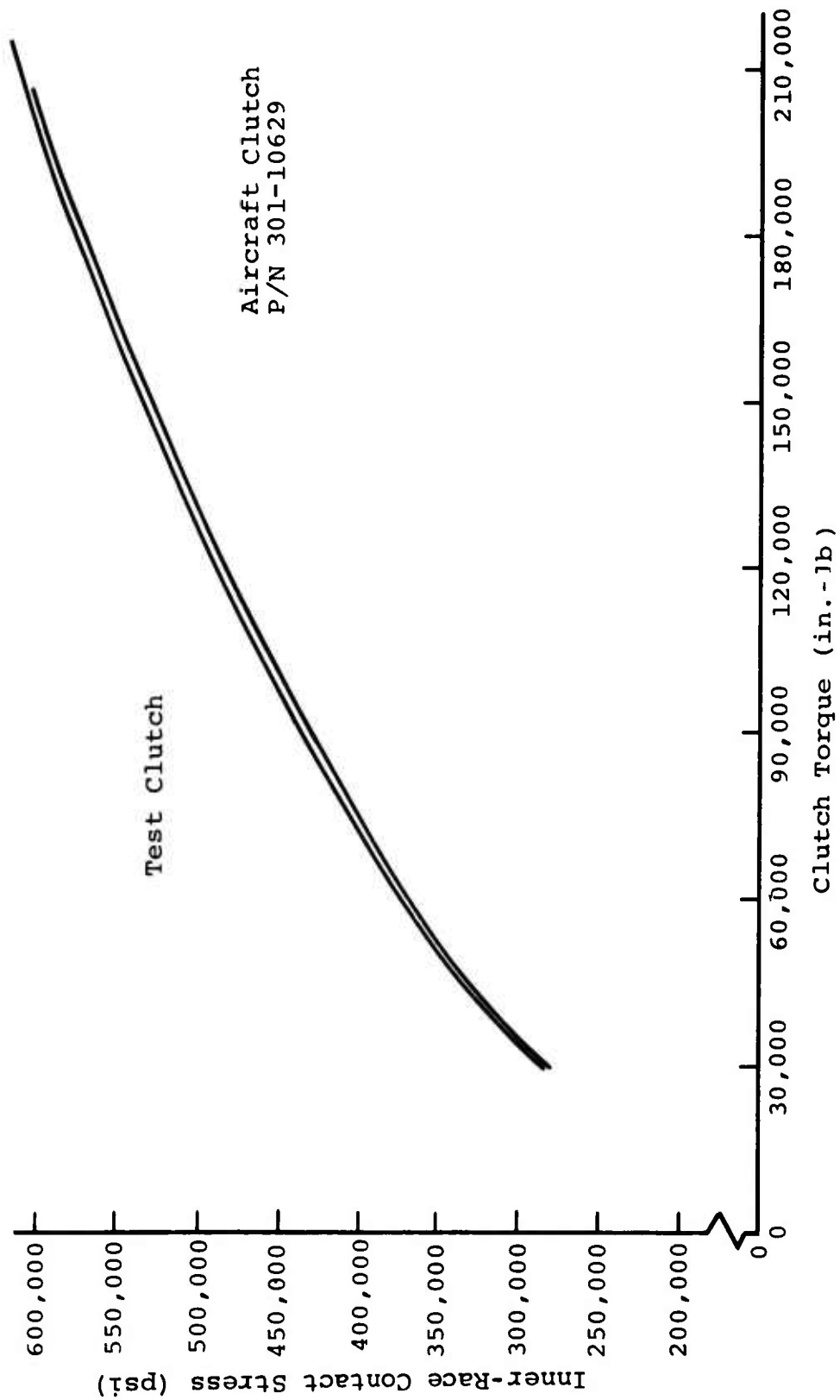


Figure 50. Inner-Race Contact Stress Versus Clutch Torque.

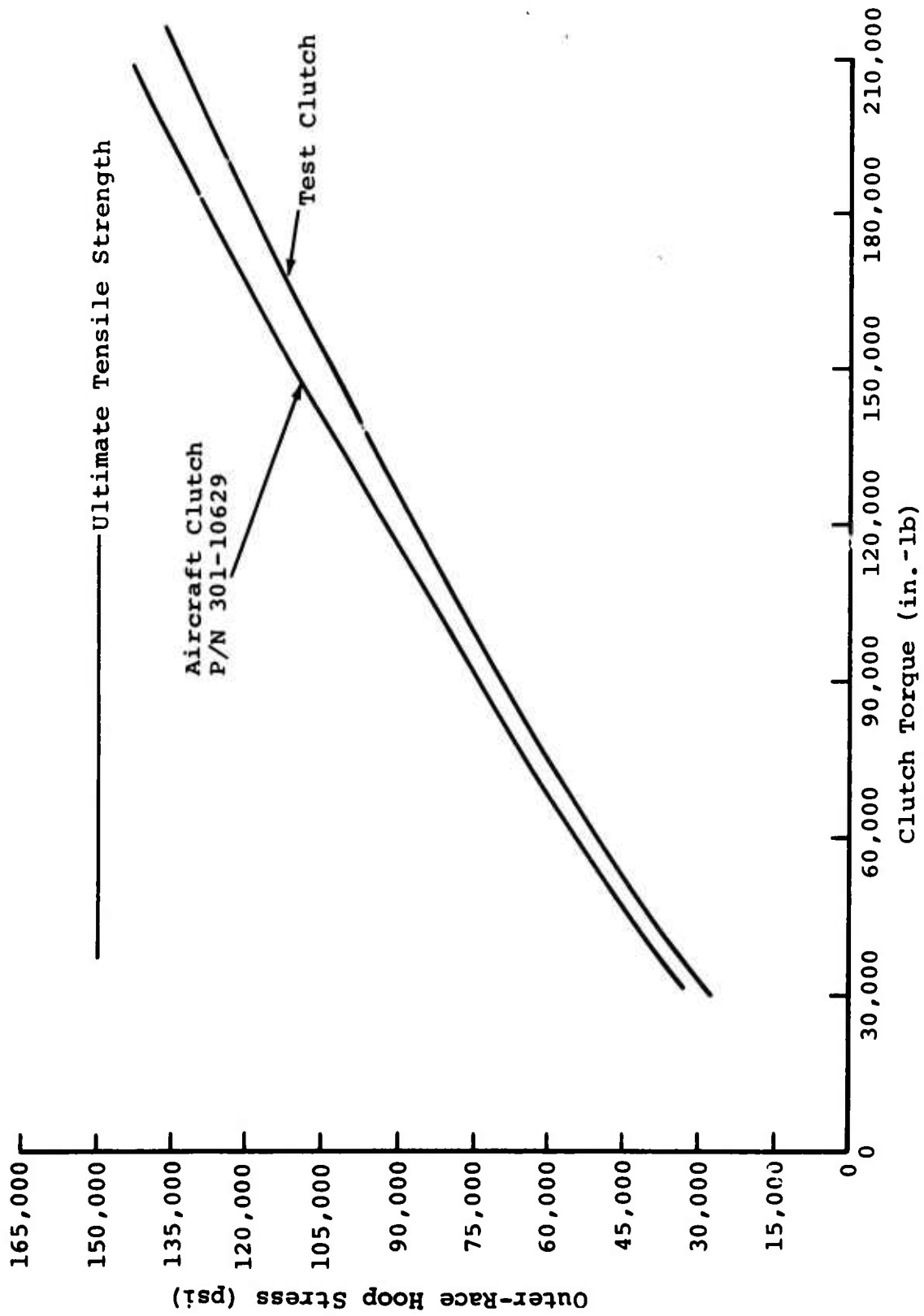


Figure 51. Outer-Race Hoop Stress Versus Clutch Torque.

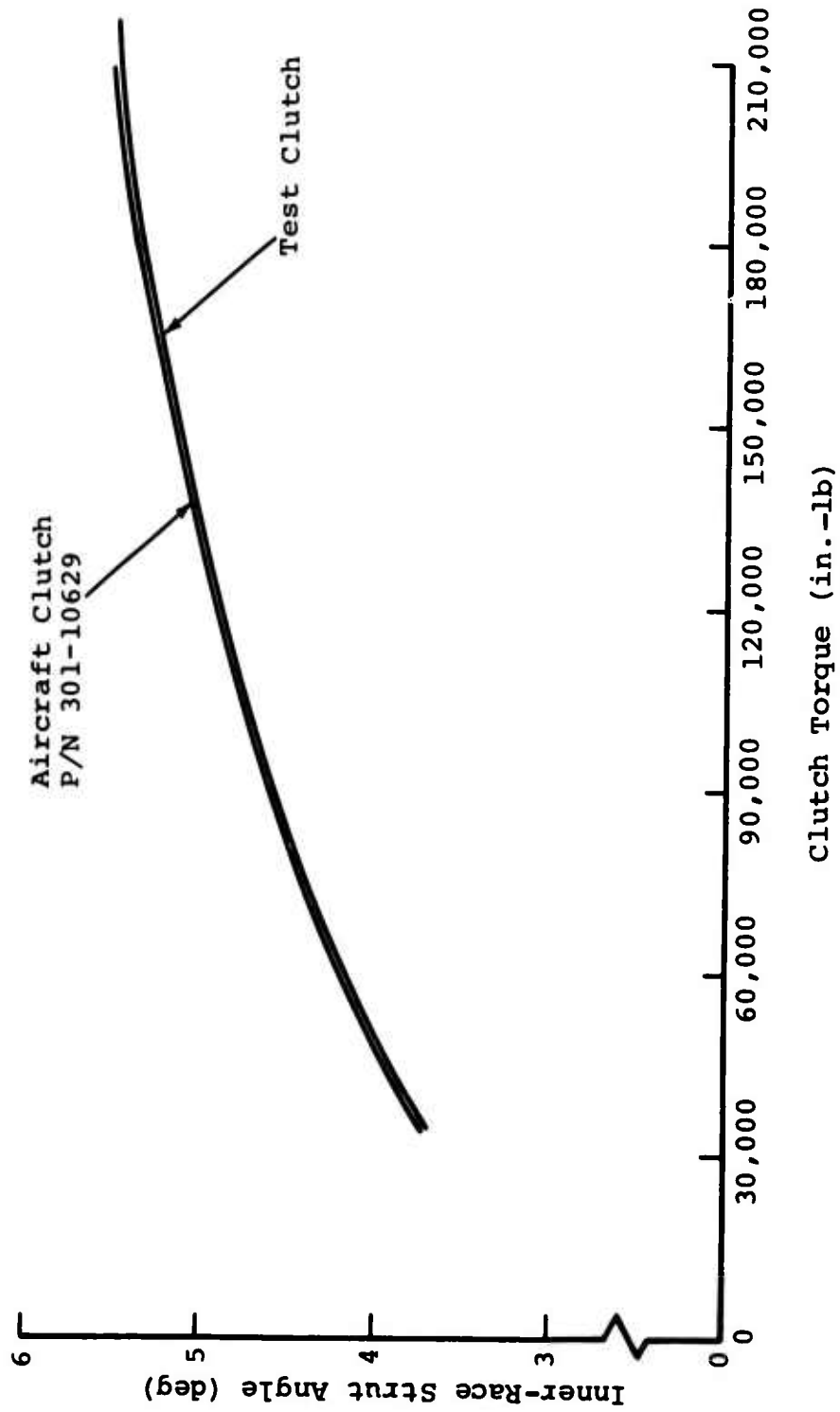
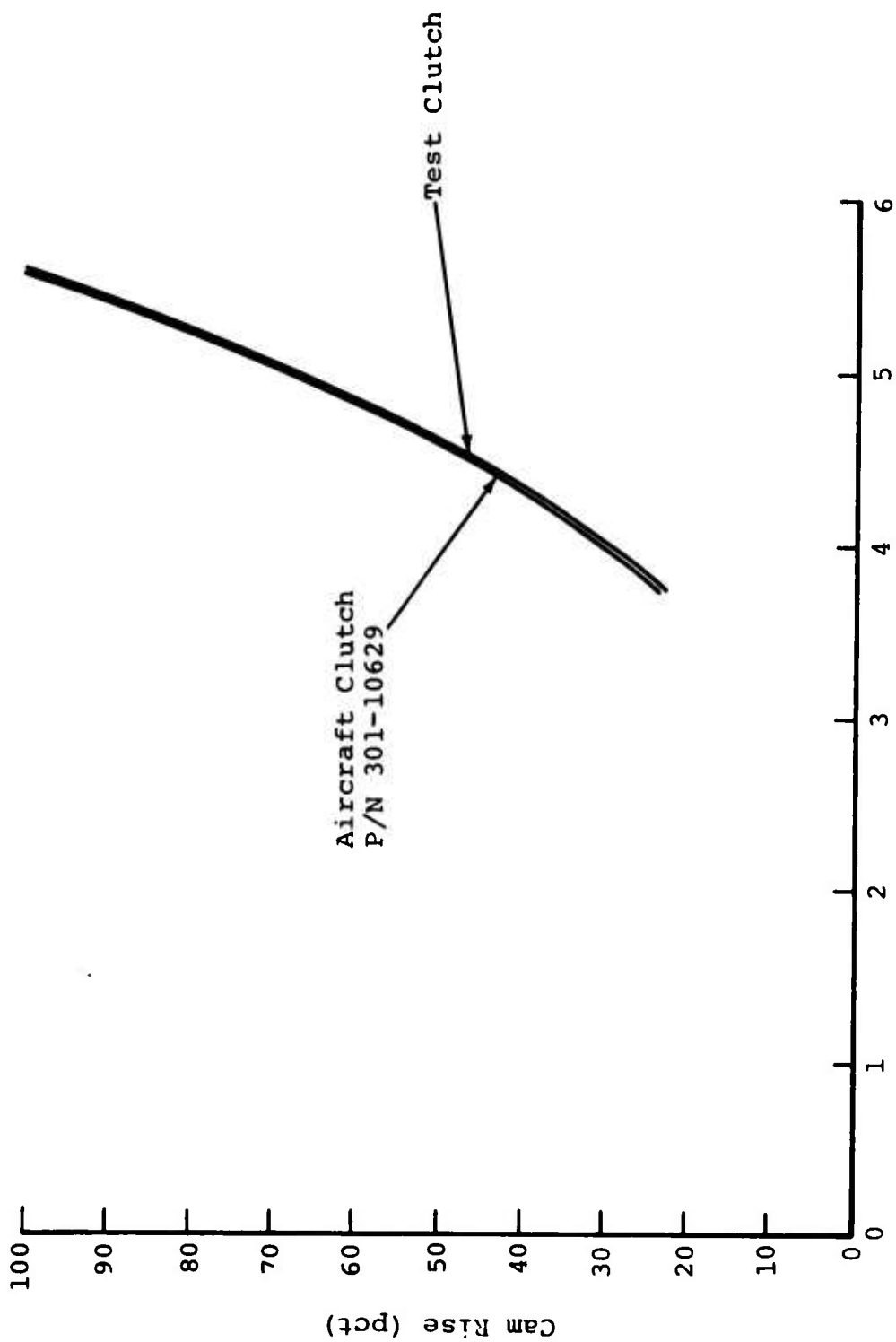


Figure 52. Inner-Race Strut Angle Versus Clutch Torque.



Inner-Race Strut Angle (deg)

Figure 53. Percentage of Cam Rise Versus Inner-Race Strut Angle.

TABLE X. COMPARISON OF DESIGN D AND AIRCRAFT CLUTCH PARAMETERS WITH DESIGN CRITERIA

Parameter	Design Criteria	Design D	HLH Clutch
Contact Stress at 200 Percent of Torque, psi	$\leq 450,000$	435,000	433,000
Contact Stress at 300 Percent of Torque, psi	$\leq 600,000$	510,000	504,000
No Failure (Rollover), pct of torque	≥ 450	489 ^a 469 ^b	466 ^a 447 ^c
Outer-Race Hoop Stress at 200 Percent of Torque, psi	$\leq 71,200$	68,400	73,600
Cam Rise at 200 Percent of Torque, pct	≤ 80	49.8	51.7
^a Calculated ^b Test ^c Estimated from test			

CONCLUSIONS

The three clutch designs evaluated successfully met all of the technical requirements of the dynamic tests with the aid of alternative parts. The clutch design and manufacturer were therefore selected on the basis of:

- Cost
- Engineering cooperation between vendor and purchaser

The clutch selected as the optimum configuration was manufactured by the Borg-Warner Company. It successfully passed all tests and met all design criteria.

The few minor discrepancies found will be eliminated by more stringent manufacturing processes and better quality-control methods.

APPENDIX SPRAG-CLUTCH ANALYSIS

The objective of this analysis is to determine the following items as functions of torque: strut angles, contact stresses, race-hoop stresses, and cam rise. In the following paragraphs the pertinent equations are derived and the method of solution is outlined.

SPRAG GEOMETRY

The basic sprag geometry is shown in Figure 54.

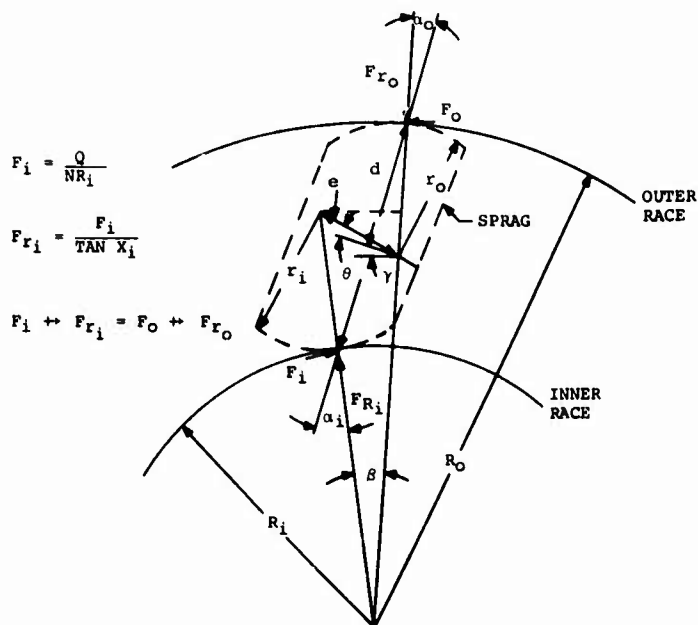


Figure 54. Sprag Geometry.

By definition, $h = R_o - R_i$. By law of cosines,

$$\cos \beta = \frac{(R_i + r_i)^2 + (R_o - r_o)^2 - e^2}{2(R_i + r_i)(R_o - r_o)}$$

$$\beta = \cos^{-1} \frac{(R_i + r_i)^2 + (R_o - r_o)^2 - e^2}{2(R_i + r_i)(R_o - r_o)}$$

$$\sin \beta = \frac{e \cos (\theta + \gamma)}{R_i + r_i}$$

$$\tan \alpha_o = \frac{R_i \sin \beta}{R_o - r_i \cos \beta}$$

$$\alpha_o = \text{TAN}^{-1} \frac{R_i \text{ SIN } \beta}{R_o - R_i \text{ COS } \beta}$$

By law of sines

$$\frac{R_o}{\text{SIN}(\pi - \alpha_i)} = \frac{R_o}{\text{SIN } \alpha_i} = \frac{R_i}{\text{SIN } \alpha_o} = \frac{d}{\text{SIN } \beta}$$

$$\alpha_i = \text{SIN}^{-1} \frac{R_o}{R_i} \text{ SIN } \alpha_o = \alpha_o + \beta$$

$$d = R_i \frac{\text{SIN } \beta}{\text{SIN } \alpha_o} = R_o \frac{\text{SIN } \beta}{\text{SIN } \alpha_i}$$

For a given sprag (r_i, r_o, e) and race (R_o, R_i) design, the strut angles at engagement can be determined. If the change in the above parameters with torque can be defined, the strut angles can also be determined as a function of torque.

INNER-RACE DEFLECTION

For a thick cylinder under uniform external pressure,

$$\delta_{oi} = P_i \frac{R_i}{E} \left[\frac{2R_i^2 - 2R_i t_i + t_i^2}{2R_i t_i - t_i^2} - v \right]$$

The sprag loads can be converted to an equivalent pressure by

$$P_i = \frac{F_{ri} N}{2\pi R_i L_e} = \frac{N}{2\pi R_i L_e} \times \frac{Q}{NR_i \text{ TAN } \alpha_i} = \frac{Q}{2\pi L_e R_i^2 \text{ TAN } \alpha_i}$$

$$\delta_{oi} = \frac{Q}{2\pi E L_e R_i \text{ TAN } \alpha_i} \left[\frac{2R_i^2 - 2R_i t_i + t_i^2}{2R_i t_i - t_i^2} - v \right]$$

For steel, $E = 29 \times 10^6$ psi; $v = .32$.

$$\delta_{oi} = \frac{.549 \times 10^{-8} Q}{R_i L_e \text{ TAN } \alpha_i} \left[\frac{2R_i^2 - 2R_i t_i + t_i^2}{2R_i t_i - t_i^2} - .32 \right]$$

$$\text{Defining } A = \frac{.549 \times 10^{-8}}{R_i L_e} \left[\frac{2R_i^2 - 2R_i t_i + t_i^2}{2R_i t_i - t_i^2} - .32 \right]$$

$$\delta_i = A \frac{Q}{\text{TAN } \alpha_i}$$

OUTER-RACE DEFLECTION

For a thick cylinder under uniform internal pressure,

$$\delta_{oo} = P_o \frac{R_o}{E} \left[\frac{2R_o^2 + 2R_o t_o + t_o^2}{2R_o t_o + t_o^2} + v \right]$$

The sprag loads can be converted to an equivalent pressure by

$$P_o = \frac{F_{r_o} N}{2\pi R_o L_e} = \frac{N}{2\pi R_o L_e} \times \frac{Q}{N R_o \text{TAN } \alpha_o} = \frac{Q}{2\pi L_e R_o^2 \text{TAN } \alpha_o}$$

Since $R_o \text{ SIN } \alpha_i = R_i \text{ SIN } \alpha_i$ and since both α_i and α_o are small angles (less than 5 degrees),

$$R_o \text{TAN } \alpha_o \cong R_o \text{TAN } \alpha_i$$

$$P_o = \frac{Q}{2\pi L_e R_o^2} \times \frac{R_o}{R_i \text{TAN } \alpha_i} = \frac{Q}{2\pi L_e R_i R_o \text{TAN } \alpha_i}$$

$$\delta_{oo} = \frac{Q}{2\pi E L_e R_i \text{TAN } \alpha_i} \left[\frac{2R_o^2 + 2R_o t_o + t_o^2}{2R_o t_o + t_o^2} + v \right]$$

For steel, $E = 29 \times 10^6$ psi; $v = .32$.

$$\delta_{oo} = \frac{.549 \times 10^{-8} Q}{R_i L_e \text{TAN } \alpha_i} \left[\frac{2R_o^2 + 2R_o t_o + t_o^2}{2R_o t_o + t_o^2} + .32 \right]$$

$$\text{Defining } B = \frac{.549 \times 10^{-8}}{R_i L_e} \left[\frac{2R_o^2 + 2R_o t_o + t_o^2}{2R_o t_o + t_o^2} + .32 \right]$$

$$\delta_o = B \frac{Q}{\text{TAN } \alpha_i}$$

SPRAG DEFLECTION

For a bar of length r_i in compression,

$$\delta_{ri} = \frac{F_{ri} r_i}{L_t s E} = \frac{r_i}{L_t s E} \times \frac{Q}{N R_i \text{TAN } \alpha_i} = \frac{r_i Q}{L_t s E N R_i \text{TAN } \alpha_i}$$

For steel, $E = 29 \times 10^6$ psi.

$$\delta_{ri} = \frac{3.45 \times 10^{-8} r_i Q}{L_t s N R_i \text{TAN } \alpha_i}$$

$$\text{Defining } C = \frac{3.45 \times 10^{-8} r_i}{L_t s N R_i}$$

$$\delta_{ri} = C \frac{Q}{\text{TAN } \alpha_i}$$

For a bar of length r_o in compression,

$$\delta_{ro} = \frac{F_{ro} r_o}{L_t s E} = \frac{r_o}{L_t s E} \times \frac{Q}{N R_o \text{TAN } \alpha_o} = \frac{r_o Q}{L_t s E N R_i \text{TAN } \alpha_i}$$

$$\delta_{ro} = \frac{3.45 \times 10^{-8} r_o Q}{L_t s N R_i \text{TAN } \alpha_i}$$

$$\text{Defining } D = \frac{3.45 \times 10^{-8} r_o}{L_t s N R_i}$$

$$\delta_{r_o} = D \frac{Q}{\text{TAN } \alpha_i}$$

SPRAG-RACE CONTACT DEFLECTION

The approach between a steel cylinder and plane is given by

$$\delta_c = .436 \times 10^{-8} \frac{P^{.9}}{L^{.8}}$$

$$\delta_{ci} = \frac{.436 \times 10^{-8}}{L^{.8}} \times F_{r_i}^{.9} = \frac{.436 \times 10^{-8}}{L^{.8}} \left[\frac{Q}{N R_i \text{TAN } \alpha_i} \right]^{.9}$$

$$\delta_{ci} = \frac{.436 \times 10^{-8}}{L^{.8} N^{.9} R_i^{.9}} \frac{Q}{\text{TAN } \alpha_i}^{.9}$$

$$\delta_{co} = \frac{.436 \times 10^{-8}}{L^{.8}} \times F_{r_o}^{.9} = \frac{.436 \times 10^{-8}}{L^{.8}} \left[\frac{Q}{N R_o \text{TAN } \alpha_o} \right]^{.9}$$

Since $R_o \text{ SIN } \alpha_o = R_i \text{ SIN } \alpha_i$ and since both α_i and α_o are small angles (less than 5 degrees), $R_o \text{ TAN } \alpha_o \approx R_i \text{ TAN } \alpha_i$.

$$\delta_{co} = \frac{.436 \times 10^{-8}}{L^{.8} N^{.9} R_i^{.9}} \left[\frac{Q}{\text{TAN } \alpha_i} \right]^{.9}$$

$$\text{Defining } H = \frac{.436 \times 10^{-8}}{L^{.8} N^{.9} R_i^{.9}}$$

$$\delta_{ci} = \delta_{co} = H \left[\frac{Q}{\text{TAN } \alpha_i} \right]^{.9}$$

CALCULATION OF STRUT ANGLE VERSUS TORQUE

For a given torque Q and an assumed inner-race strut angle α_i , the change in the dimensions r_i , r_o , R_i , and R_o can be determined by the methods of the preceding paragraph.

Letting the primes denote deflected dimensions and defining

$$x = \frac{Q}{\text{TAN } \alpha_i} :$$

$$r'_i = r_i - Cx - \frac{H}{2} x^{.9}$$

$$r'_o = r_o - Dx - \frac{H}{2} x^{.9}$$

$$R'_i = R_i - Ax - \frac{H}{2} x^{.9}$$

$$R'_o = R_o + Bx + \frac{H}{2} x^{.9}$$

With the deflected dimensions and the method for determining deflections, the contact angle β' and thus the inner-race strut angle α'_i can be determined. The solution can be obtained by iterating until the initially assumed α_i is equal to that resulting from the calculation.

SPRAG-RACE CONTACT STRESSES

$$S_{ci} = .798 \left[\frac{F r_i E (2R_i + 2r_i)}{2L(1-v^2) (2R_i) (2r_i)} \right]^{1/2} = .399 \left[\frac{QE (R_i + r_i)}{LNR_i^2 \text{TAN } \alpha_i (1-v^2)} \right]^{1/2}$$
$$S_{co} = .798 \left[\frac{F r_o E (2R_o - 2r_o)}{2L(1-v^2) (2R_o) (2r_o)} \right]^{1/2} = .399 \left[\frac{QE (R_o - r_o)}{LNR_o^2 \text{TAN } \alpha_o (1-v^2)} \right]^{1/2}$$

For steel, $E = 29 \times 10^6$ psi; $v = .32$. And since $R_o \text{ TAN } \alpha_o \approx R_i \text{ TAN } \alpha_i$,

$$S_{ci} = 2268 \left[\frac{R_i + r_i}{\text{LN } r_i R_i^2} \times \frac{Q}{\text{TAN } \alpha_i} \right]^{1/2}$$

$$S_{co} = 2268 \left[\frac{R_o - r_o}{\text{LN } r_o R_i R_o} \times \frac{Q}{\text{TAN } \alpha_i} \right]^{1/2}$$

RACE STRESSES

For a thick cylinder under uniform external pressure,

$$S_i = 2p_i \frac{R_i^2}{2R_i t_i - t_i^2}$$

$$\text{Since } p_i = \frac{Q}{2\pi L R_i^2 \text{TAN } \alpha_i}$$

$$S_i = \frac{1}{\pi L (2R_i t_i - t_i^2)} \times \frac{Q}{\text{TAN } \alpha_i}$$

For a thick cylinder under uniform internal pressure,

$$S_o = p_o \frac{2R_o^2 + 2R_o t_o + t_o^2}{2R_o t_o + t_o^2}$$

$$\text{Since } p_o = \frac{Q}{2\pi L R_o^2 \text{TAN } \alpha_o}$$

$$\text{and } R_o \text{TAN } \alpha_o \cong R_i \text{TAN } \alpha_i$$

$$S_o = \frac{2R_o^2 + 2R_o t_o + t_o^2}{2\pi L R_o R_i (2R_o t_o + t_o^2)} \times \frac{Q}{\text{TAN } \alpha_i}$$

CAM RISE

$$CR = \delta_o + \delta_i + \delta_{r_o} + \delta_{r_i} + \delta_{c_o} + \delta_{c_i}$$

$$\text{Percentage cam rise} = \frac{ACR}{CR} \times 100$$

Clutch rollover occurs when the cam rise is 100 percent of the available cam rise.

LIST OF SYMBOLS

ACR	available cam rise, in.
CR	actual cam rise, in.
E	modulus of elasticity, psi
e	offset between centers of r_i and r_o , in.
h	sprag height, in.
L	sprag contact length, in. (If clutch contains two rows, L is twice the length of each sprag.)
Le	effective sprag length (1.05L), in.
N	number of sprags per row
Q	clutch torque, in.-lb
R	race radius, in.
r	sprag cam radius, in.
S	race circumferential (hoop) stress, psi
S_c	sprag-race contact stress, psi
t	race thickness, in.
t_s	sprag thickness, in.
v	Poisson's ratio
α	strut angle, deg
β	contact angle, deg

Subscripts

i	inner race
o	outer race